Trans-eQTL mapping prioritises *USP18* as a negative regulator of interferon response at a lupus risk locus

Krista Freimann[1,2], Anneke Brümmer[3,4], Robert Warmerdam[5,6], Tarran S. Rupall[2,7], Ana Laura Hernández-Ledesma[8], Joshua Chiou[9], Emily R. Holzinger[10], Joseph C. Maranville[10], Nikolina Nakic[11], Halit Ongen[12], Luca Stefanucci[2,7], Michael C. Turchin[10], eQTLGen Consortium[†], Lude Franke[5,6], Urmo Võsa[13], Carla P. Jones[2,7], Alejandra Medina-Rivera[8], Gosia Trynka[2,7], Kai Kisand[14], Sven Bergmann[3,4,15], Kaur Alasoo[1,2*]

1. Institute of Computer Science, University of Tartu, Tartu, Estonia
2. Open Targets, South Building, Wellcome Genome Campus, Hinxton, Cambridge, UK
3. Department of Computational Biology, University of Lausanne, Switzerland
4. Swiss Institute of Bioinformatics, Lausanne, Switzerland
5. Department of Genetics, University of Groningen, University Medical Center Groningen, Groningen, the Netherlands
6. Oncode Institute, Amsterdam, the Netherlands
7. Wellcome Sanger Institute, Wellcome Genome Campus, Hinxton, UK
8. Laboratorio Internacional de Investigación Sobre el Genoma Humano, Universidad Nacional Autónoma de México, Santiago de Querétaro, Mexico
9. Internal Medicine Research Unit, Research and Development, Pfizer, Cambridge, MA, USA
10. Bristol Myers Squibb, Cambridge, Massachusetts, USA
11. Research Technologies, GSK, Stevenage, UK
12. Research Technologies, GSK, Heidelberg, Germany
13. Institute of Genomics, University of Tartu, Tartu, Estonia
14. Institute of Biomedicine and Translational Medicine, Faculty of Medicine, University of Tartu, Estonia
15. Department of Integrative Biomedical Sciences, University of Cape Town, Cape Town, South Africa

[†]A list of authors and affiliations for the eQTLGen Consortium is listed in the Supplementary Materials.

[*]Corresponding author. Email: kaur.alasoo@ut.ee

Abstract

Although genome-wide association studies have provided valuable insights into the genetic basis of complex traits and diseases, translating these findings to causal genes and their downstream mechanisms remains challenging. We performed *trans* expression quantitative trait locus (*trans*-eQTL) meta-analysis in 3,734 lymphoblastoid cell line samples, identifying four robust loci that replicated in an independent multi-ethnic dataset of 682 individuals. We prioritised a missense variant in the ubiquitin specific peptidase 18 (*USP18)* gene that is a known negative regulator of interferon signalling and has previously been associated with increased risk of systemic lupus erythematosus (SLE). The SLE risk allele increased the expression of 50 interferon-inducible genes, suggesting that the risk allele impairs USP18's

ability to effectively limit the interferon response. Intriguingly, the *USP18 trans*-eQTL signal would not have been discovered in a meta-analysis of up to 43,301 whole blood samples, reaffirming the importance of capturing context-specific genetic effects for GWAS interpretation.

Introduction

Genome-wide association studies (GWAS) have provided valuable insights into the genetic basis of complex traits and diseases. However, translating GWAS findings to actionable drug targets has remained challenging, particularly when the functions of the associated genes are unknown. A promising technique to identify the effector genes of GWAS variants as well as their downstream regulatory consequences is *trans* gene expression and protein quantitative trait loci (*trans*-QTL) analysis. *Trans*-QTL studies test for association between genetic variants across the genome and expression levels of all measured genes or proteins[1]. In a prominent example, an erythrocyte-specific regulatory element first identified as a *trans* protein QTL (*trans*-pQTL) for foetal haemoglobin (HbF) was used to design the first ever gene editing therapy for sickle-cell disease[2,3].

Trans-QTLs are especially promising, because 60%-90% of gene and protein expression heritability is located in *trans*[4], most associations detected in large-scale pQTL studies are located in *trans*[5], and *cis*-QTL discovery is starting to saturate after 10,000 samples[5]. Furthermore, most complex trait heritability has been proposed to be mediated by *trans*-QTL effects[4]. However, current large-scale *trans*-eQTL and *trans*-pQTL studies have been limited to easily accessible bulk tissues such as whole blood[6,7] or plasma[5,8–10]. Bulk tissue studies are subject to cell type composition effects which can be difficult to distinguish from true intracellular *trans*-QTLs[1,6]. The whole blood and plasma studies are also likely to miss cell type and context specific regulatory effects. In contrast, *trans*-eQTL studies in other tissues and purified cell types have had limited statistical power due to small sample sizes (typically less than one thousand samples), enabling the discovery of only very large effects and potentially underestimating pleiotropic effects on multiple target genes[11–18].

A key limitation in our understanding of how *trans*-eQTLs contribute to complex traits and how they interact with *cis*-eQTL is the lack of well-characterised disease-associated *trans*-eQTL signals[4]. Two most prominent examples include the adipose-specific *KLF14* locus associated with type 2 diabetes[16,19] and the IRX3/5 locus associated with obesity[20,21]. At the *KLF14* locus, the lead variant (rs4731702) is a *cis*-eQTL for the *KLF14* transcription factor and was associated with the expression of 385 target genes in *trans*, 18 of which also had independent *cis* associations for other metabolic traits[19]. The simultaneous regulation of multiple target genes in *trans*-eQTL regulatory networks seems to be a general property of many known *trans*-eQTL signals[6,12,14]. However, what proportion of *trans*-eQTL target genes directly mediate the disease or trait associations as opposed to being independent ‘bystanders’ with minimal direct causal effect has remained unclear.

We performed the largest *trans*-eQTL meta-analysis in a single cell type, comprising 3,734 lymphoblastoid cell line (LCL) samples across nine cohorts (MetaLCL). LCLs are obtained by

transforming primary B-cells with Epstein-Barr virus[22]. LCLs have been widely used as a resource for human genetics, from banking cells from rare genetic disorders, through control material in laboratories to prevent repetitive blood sampling, to the study of tumorigenesis, mechanisms of viral latency and immune evasion[22]. Furthermore, Epstein-Barr virus has been epidemiologically linked to several autoimmune diseases in which B cells are implicated to play a pathogenic role, such as multiple sclerosis (MS)[23,24] and systemic lupus erythematosus (SLE)[25] with recent studies starting to elucidate the potential molecular mechanisms underlying these associations[26–28]. Thus, *trans*-eQTLs discovered in LCLs might provide insights into the pathogenesis of these autoimmune diseases, especially in the context of chronic exposure to viral stimuli.

After stringent quality control, we identified four highly robust *trans*-eQTL associations that replicated in an independent cohort (n=682) and were associated with multiple target genes. One of these signals corresponded to a prioritised missense variant in the *USP18* gene and was also associated with increased risk of SLE. The SLE risk allele was associated with increased activity of the type I interferon signalling pathway and increased expression of several classical interferon response genes. While there is robust evidence for the potential causal role of increased interferon signalling in SLE pathogenesis, we find that the expression of many individual interferon response genes is unlikely to have a direct causal effect on SLE. Our results caution against blindly using *trans*-QTL associations for target gene prioritisation without clear understanding of the *trans*-QTL mechanism and robust genetic evidence from *cis*-acting variants implicating the same gene. To support secondary use of our data, we have made the complete MetaLCL *cis* and *trans*-eQTL summary statistics for 18,792 genes publicly available via the eQTL Catalogue FTP server.

Results

Large-scale *trans*-eQTL meta-analysis in a single cell type

We performed a large-scale *trans*-eQTL meta-analysis, utilising data from LCLs collected from 3,734 donors across nine cohorts of European ancestries (Figure 1A, Table S1). After excluding *cis* associations located within 5 Mb of the target gene, we identified 79 suggestive independent *trans*-eQTL loci at p-value < $1x10^{-11}$ threshold (Figure 1B). To identify robust signals associated with multiple target genes and reduce the risk of false positives caused by cross-mappability[29], we further required each locus to be associated with at least five independent target genes (p < $5x10^{-8}$) with low cross-mappability scores (see Methods). This filtering reduced the number of candidate loci to six (Figure 1B), four of which replicated in an independent multi-ethnic cohort of 682 individuals[30]. These four replicating *trans*-eQTL loci were located near the *BATF3*, *MYBL2*, *USP18*, *HNF4G* genes (Table S2, Figure S2). While the strong *trans*-eQTL signal near the *BATF3* transcription factor (2294 targets at FDR 5%) has been previously reported[31], the other three seem to be novel. Remarkably, the *trans*-eQTL targets at the *MYBL2* locus were consistent with direct activation by the MYBL2 transcription factor (Supplementary Note), indicating that our analysis is identifying biologically interpretable signals.

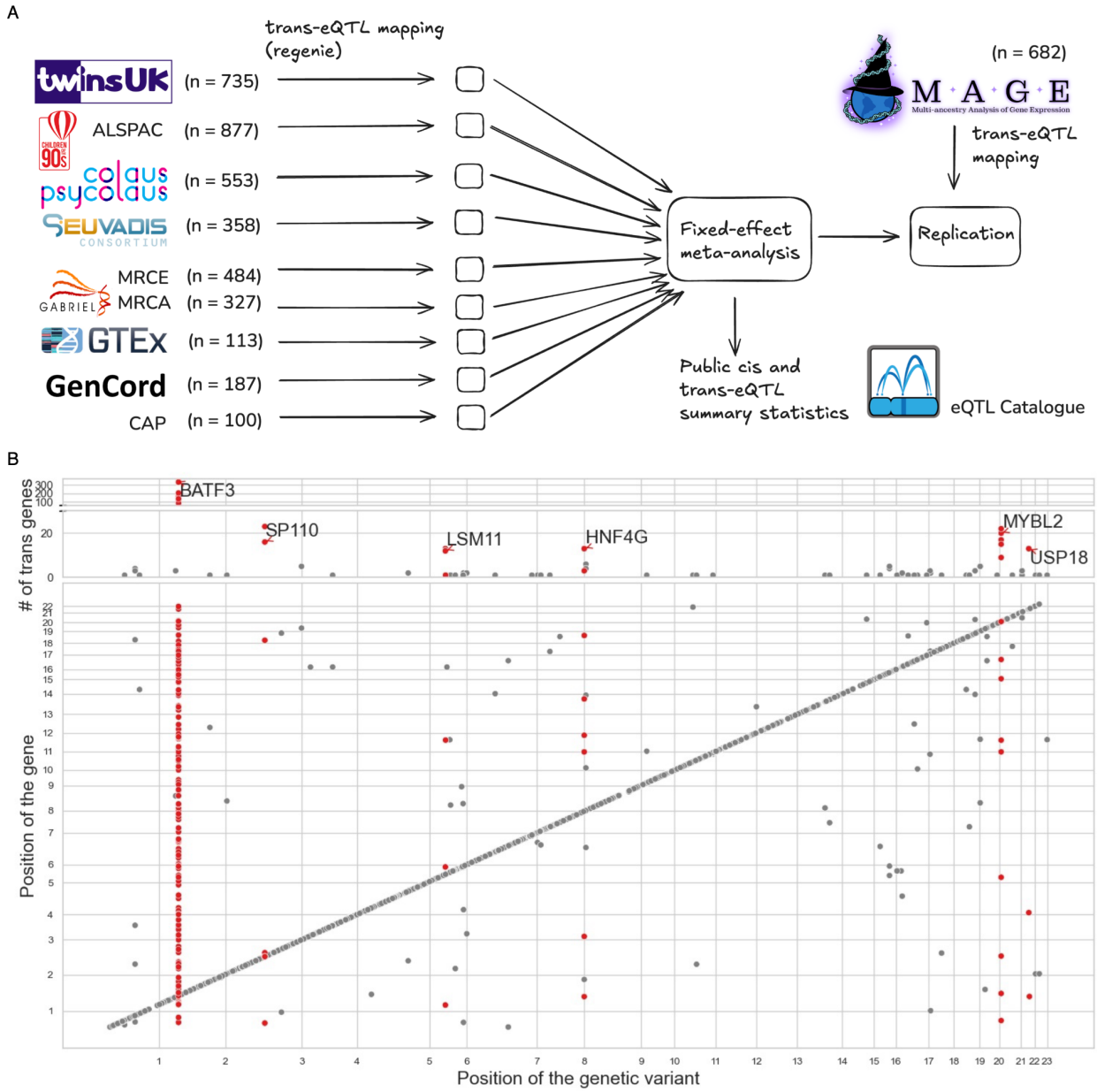

Figure 1. Overview of the MetaLCL study. (A) Overview of the study design. **(B)** Significant *trans*-eQTLs detected in the meta-analysis. The upper scatter plot shows the number of *trans* associations detected at each *trans*-eQTL locus with p-values < $5x10^{-8}$. Six largest *trans*-eQTL loci have been labelled with the name of the closest *cis* gene. The lower scatter plot shows all significant loci for each tested gene at the more stringent p < $1x10^{-11}$ threshold. *Cis* associations are located on the diagonal while putative *trans* associations are located off diagonal.

USP18 is a negative regulator of interferon response at a lupus GWAS locus

For the four high-confidence loci, we performed GWAS lookup using the Open Targets Genetics Portal[32] and found that only the *USP18* locus lead variant (chr22_18166589_T_C, rs4819670)

was in high LD (r2 > 0.9) with an annotated GWAS hit. Specifically, the *USP18* lead variant was identical to a GWAS lead variant reported for SLE in East Asians[33]. Using the point estimation of colocalisation (POEMColoc) method, we confirmed that the two signals colocalised (PP4 = 0.97) (Figure 2A)[34]. At this locus, we identified 40 *trans* target genes at FDR 5% that were all strongly enriched for Reactome interferon signalling (R-HSA-913531, $p = 1.1 \times 10^{-26}$) and interferon alpha/beta signalling (R-HSA-909733, $p = 1.7 \times 10^{-21}$) pathways. The rs4819670-C allele was associated with decreased expression of multiple canonical type I interferon response genes (e.g. *ISG15*, *IFI44*, *OAS1-3*) (Figure 2B). Reassuringly, we observed consistent effect sizes across nine sub-cohorts in our meta-analysis (I^2 heterogeneity statistic = 0.46, Figure S2). The rs4819670-C was also associated with decreased risk of systemic lupus erythematosus (SLE) in East Asians[33].

We next sought to identify the most likely causal gene at the *USP18* locus. Since the *trans*-eQTL effect was detected in cultured LCLs, this implies that the causal *cis* effect mediating the *trans* associations must also be present in the same cell type (i.e. it cannot be mediated by a *trans*-acting factor such as a cytokine produced by some other cell type). Although the rs4819670 variant was located in an intron of *USP18*, we did not detect a significant *cis*-eQTL effect for USP18 or any other neighbouring genes neither in our meta-analysis nor the full eQTL Catalogue release 6[35]. We also did not detect a splicing QTL for *USP18* or other neighbouring genes in eQTL Catalogue release 6. However, the rs4819670 lead variant was in high linkage disequilibrium (LD) with a *USP18* missense variant rs3180408 (chr22_18167915_C_T, ENSP00000215794.7:p.Thr169Met) in both European and East Asian populations ($r^2 = 1$ in EAS and $r^2 = 0.96$ in EUR 1000 Genomes superpopulation). Furthermore, *USP18* is a known negative regulator of interferon signalling and a rare loss-of-function mutation in *USP18* causes severe type I interferonopathy (Figure 2C)[36,37]. These results indicate that *USP18* is the most likely causal gene at this *trans*-eQTL locus and the absence of *cis* eQTL and splicing QTL evidence suggest that the likely causal mechanism is the missense variant. However, the rs4819670 missense variant is predicted to be benign by all tested variant effect prediction tools available from Ensembl VEP[38]. Thus, further experimental work is required to confirm the exact function consequences of the rs3180408 missense variant at the protein level.

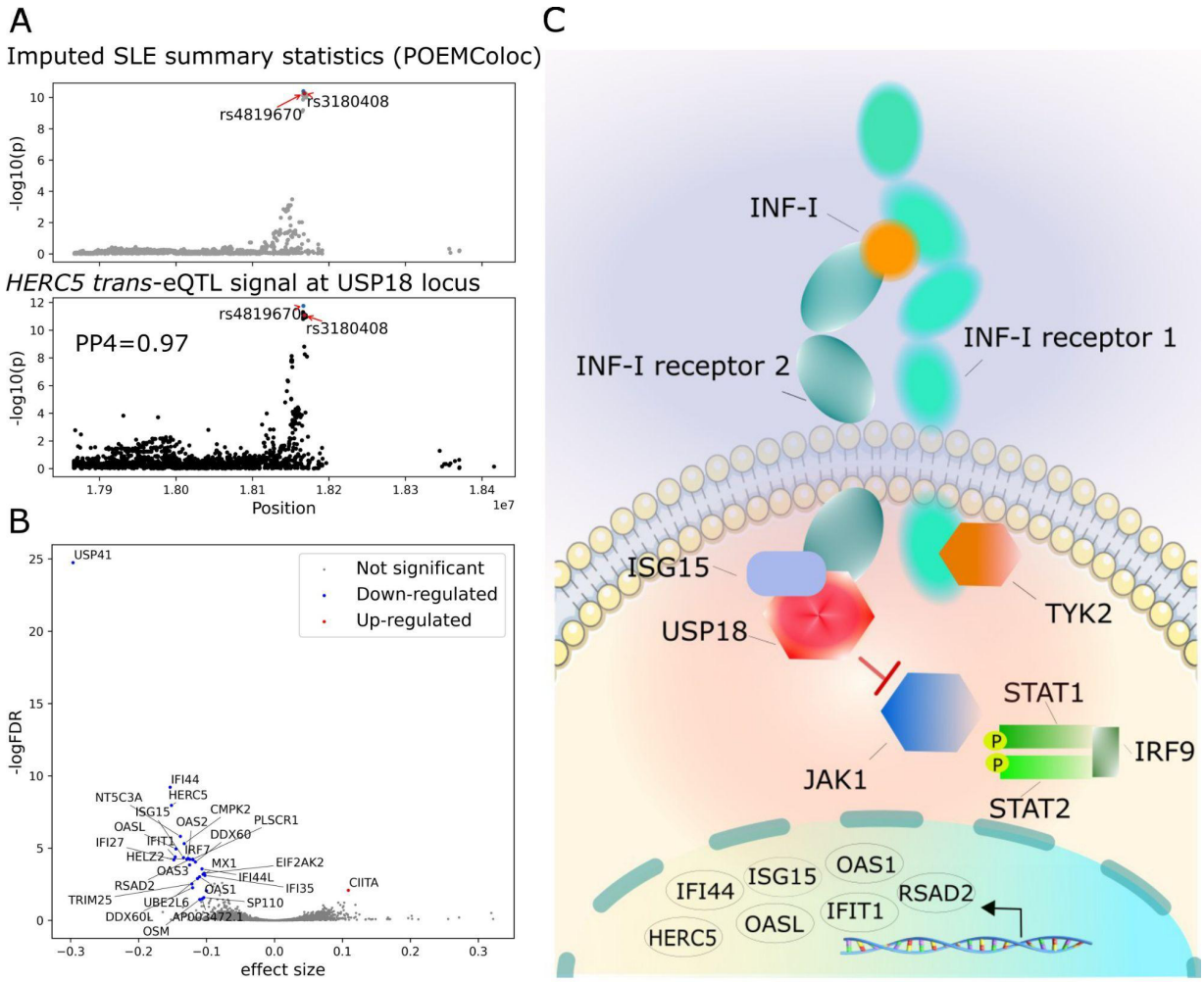

Figure 2. **SLE GWAS association at the *USP18* locus is a *trans*-eQTL for interferon response genes.** (**A**) Regional association plot for the SLE GWAS with POEMColoc imputed summary statistics and regional association plot for the lead *trans*-eQTL gene (*HERC5*) at the USP18 locus. The *trans*-eQTL lead and GWAS lead variants (rs4819670, shown in blue) are identical and in high LD with a missense variant (rs3180408, shown in red) in the *USP18* gene. The original regional association plot for the SLE GWAS is shown on Figure S4. (**B**) Volcano plot of the *trans*-eQTL target genes. (**C**) USP18 down-regulates type I interferon signalling by restricting the access of Janus-associated kinase 1 (JAK1) to the type I interferon receptor. Illustration adapted from Alsohime *et al*[37].

Role of aberrant interferon signalling in lupus pathogenesis

Several studies have suggested that causal GWAS genes are enriched in shared pathways or biological processes[39–41]. To further characterise the potential role of USP18 target genes in lupus, we performed additional *trans*-eQTL meta-analysis across the nine discovery cohorts and one replication cohort (total n = 4,416). This increased the number of significant USP18 target genes to 50 (FDR < 5%). Notably, 18/50 target genes overlapped the Reactome interferon alpha/beta signalling (R-HSA-909733) pathway (hypergeometric test, $p = 4.14 \times 10^{-24}$) and 26/50

genes overlapped a consensus set of interferon response genes (n = 124) identified by Mostafavi *et al*[42] ($p = 1.44x10^{-39}$, Table S4). Reassuringly, 39/50 genes were also more highly expressed in peripheral blood mononuclear cells from SLE cases compared to controls[43] (Table S4), consistent with the established role of increased interferon signalling in SLE[44].

To better understand the role of the USP18 target genes in the interferon alpha/beta signalling pathway, we focussed on the 60 genes belonging to the Reactome R-HSA-909733 interferon alpha/beta signalling pathway and divided them into three categories - category I: proteins involved in signal transduction via IFNAR1/2 receptor (n = 13 genes, including the multi-gene interferon-alpha gene cluster, Figure 3A); category II: downstream transcriptional targets of the interferon signalling (38 genes from the Reactome R-HSA-1015702 sub-pathway, Figure 3B) and 3) and category III: other pathway genes (n = 9) not belonging to the first two categories (Figure S5). We found that 16/50 USP18 targets were shared with the 38 category II genes (transcriptional targets of interferon response) ($p = 1.18x10^{-29}$). In contrast, only 2/50 USP18 *trans*-eQTL target genes (*STAT1* and *ISG15*) were shared with the 13 category I genes (IFNAR1/2 receptor signal transduction proteins) and were shared with the 9 category III genes. This suggests that the USP18 *trans*-eQTLs are primarily capturing the transcriptional targets of interferon response (category II), consistent with the established role of USP18 in regulating these genes (Figure 2C)[37].

Next, we assessed if there were additional lupus GWAS signals overlapping the three categories of interferon response genes defined above. We first used the Open Targets Genetics portal to extract the prioritised target genes for 108 lupus GWAS loci from Yin *et al*[33]. This revealed that three prioritised lupus genes (*USP18*, *STAT1*, *IFNA1-17)* were shared with the 13 category I genes (IFNAR1/2 signal transduction proteins, Figure 3A) and four prioritised genes (*IRF1/5/8* and *OAS1)* were shared with the 38 category II genes (transcriptional targets of interferon response, Figure 3B). Out of these, IRF1/5/8 are themselves transcription factors involved in the regulation of interferon production[45,46], and stronger IRF1 binding across many GWAS loci has been associated with higher Crohn's disease risk[47]. *OAS1* represents a classical antiviral gene and here the SLE GWAS lead variant is in perfect LD with a fine-mapped splice QTL for *OAS1* in the eQTL Catalogue (Figure S6)[35]. The consequences of this splice variant have been extensively studied in the context of Sjögren's syndrome and COVID-19 hospitalisation[48,49]. Unfortunately, we were not able to check if there were additional sub-threshold hits for lupus near the interferon alpha/beta signalling pathway genes, because the genome-wide summary statistics from Yin *et al*[33] were not available.

We also overlapped interferon alpha/beta signalling pathway genes with ongoing or completed phase III clinical trials for SLE extracted from the ChEMBL database[50]. We identified three category I (interferon signal transduction) genes (*IFNAR1*, *JAK1* and *TYK2*) that have been targeted by a clinical trial for SLE (Figure 3A). While the trials targeting *JAK1* and *TYK2* are currently ongoing, a randomised control trial of anifrolumab, a human monoclonal antibody to type I interferon receptor subunit 1 (*IFNAR1)*, found it to be an effective treatment for SLE[51]. None of the category II genes (transcriptional targets of interferon signalling, Figure 3B) and category III genes (Figure S5) are currently in a phase III clinical trial for SLE (Figure 3B).

There is an emerging consensus that rare mutations in genes prioritised for autoimmune diseases from GWAS studies can often also cause primary immunodeficiencies (PIDs)[52–54]. For example, loss-of-function mutations in *USP18* cause rare type I interferonopathy[36,37]. At the same time, GWAS studies for SLE and other autoimmune diseases are still only powered to detect variants with large effects. Thus, knowing if a gene causes PID might be a useful (if noisy) indicator that the same gene might be discovered in a future larger autoimmune GWAS study. We obtained the list of genes causing either PID or monogenic inflammatory bowel disease from Genomics England[55] and overlapped those with the three categories of interferon response genes defined above. We found that 10/13 category I genes (interferon signal transduction) have previously been implicated in causing PID, including *USP18* and all three phase III drug candidates for SLE (Figure 3A). In contrast, only 8 of the 38 category II genes (transcriptional targets of interferon response) have been implicated in PIDs (Figure 3B), including *OAS1* and IRF8 also detected by SLE GWAS. Finally, none of the category III genes have been implicated in PIDs (Figure S5).

Triangulation of evidence from prioritised lupus GWAS target genes, phase III clinical trial information and overlap with primary immunodeficiency genes reaffirms modulation of aberrant interferon alpha/beta signalling in B-cells as an emerging therapeutic opportunity for SLE (category I, Figure 3A)[54,56]. This is further supported by recent studies demonstrating that depleting autoreactive B-cells via anti-CD19 CAR T cell therapy is an effective therapy for SLE and other autoimmune diseases[57,58]. In contrast, most *trans*-eQTL targets of USP18 are transcriptional targets of interferon response (category II, Figure 3B) and it is far less clear what is the potential causal roles of these genes in SLE pathogenesis.

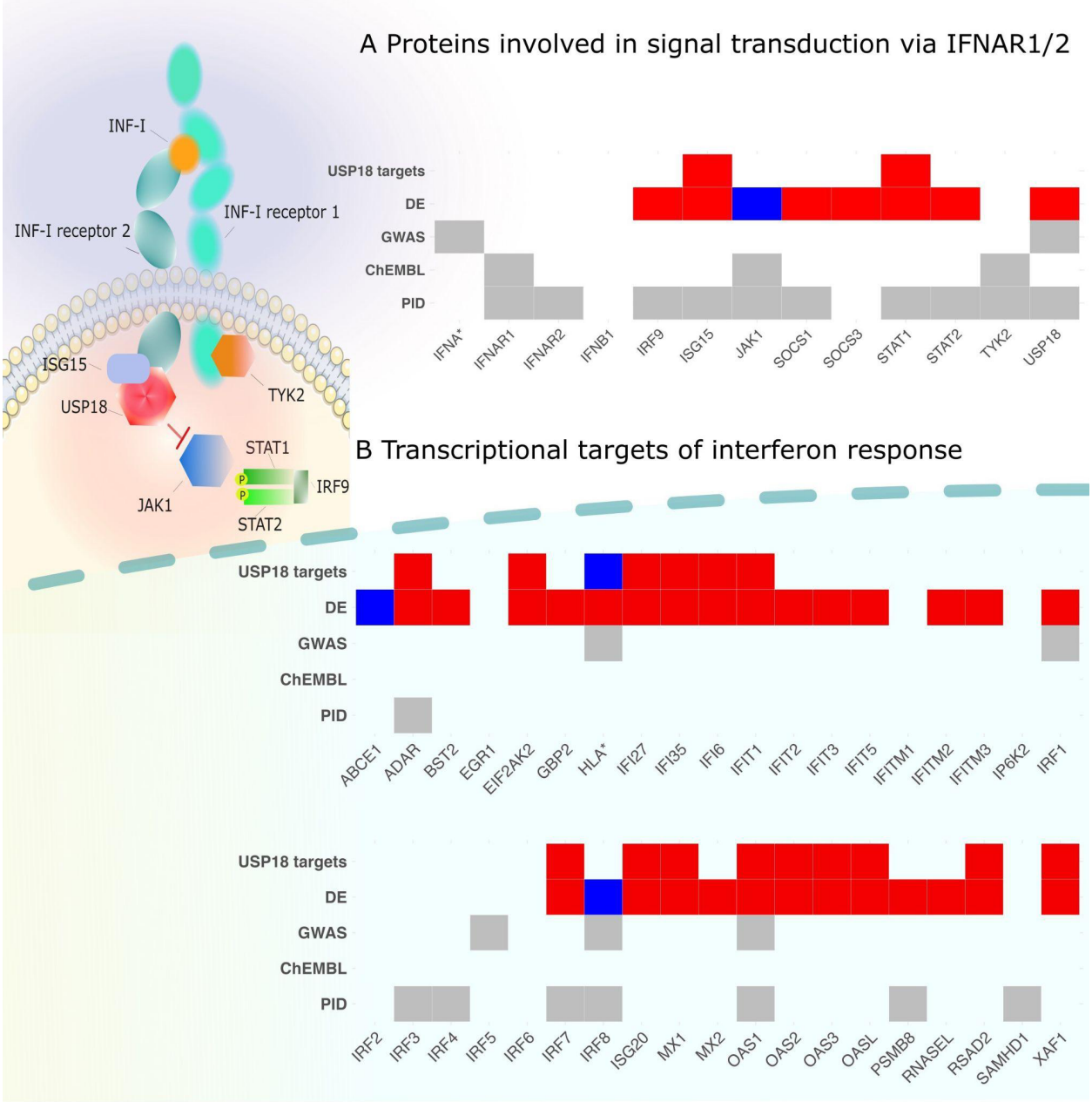

Figure 3. Role of interferon signalling in SLE pathogenesis. (**A**) Upstream regulators of interferon response genes (IFNA* contains multi-gene interferon-alpha gene cluster). (**B**) Downstream transcriptional targets of the interferon signalling (HLA* marks the HLA region). The increased gene expression is marked in red, while reduced gene expression is marked in blue. The visualisation illustrates the effect on USP18 target genes in relation to the SLE risk allele. DE - differential gene expression in SLE cases *versus* controls[43]; GWAS - GWAS hits for SLE[33], ChEMBL, phase III - SLE phase III clinical trials from ChEMBL[50], PID - genes causing primary immunodeficiency from Genomics England.

Replication of the *USP18 trans*-eQTL signal in whole blood

To understand the context-specificity of the *USP18 trans*-eQTL signal, we performed additional replication in the eQTLGen Phase 2 *trans*-eQTL meta-analysis of up to 43,301 whole blood samples. We observed that the *USP18* missense variant rs3180408 was nominally associated ($p < 0.05$) with the expression of 7/50 USP18 target genes, including our lead target gene *HERC5* ($p = 0.037$) as well as canonical interferon response genes *IFI44* and *ISG15* (Table S5). For 6/7 nominally significant associations, the effect direction was concordant between the LCL and whole blood meta-analyses, but the effect size was an order of magnitude smaller in whole blood (Table S5). Thus, even at this very large sample size, the *USP18 trans*-eQTL signal would not have been discovered in whole blood.

To understand the potential reasons for the attenuated effect in whole blood, we compared the expression level of the *USP18* gene across 49 GTEx tissues. We found that *USP18* had the highest expression in LCLs (median transcripts per million (TPM) = 45.3) and one of the lowest in whole blood (median TPM = 0.46). Since *USP18* is itself an interferon response gene and LCLs are characterised by a strong interferon signature driven by active infection with the Epstein-Barr virus, we characterised the expression of *USP18* in naive B-cells as well as B-cells stimulated with interferon-alpha and TLR7/8 agonist R848 for 16, 40 and 64 hours. We found that the expression level of *USP18* in B-cells was upregulated by ~3.5-fold after 16 hours of stimulation and stayed elevated for at least 64 hours (Figure S7). This suggests that the very strong active interferon signalling and associated upregulation of *USP18* transcription in LCLs is required for the *trans*-eQTL signal to be detected.

Discussion

We performed the largest *trans*-eQTL study in a single cell type where we profiled the expression of 18,792 genes in 3,737 individuals from nine cohorts. We then replicated these findings in an independent multi-ancestry LCL cohort of 682 individuals. After careful quality control, we identified six independent loci that were associated with five or more target genes, and that were unlikely to be driven by cross-mappability artefacts. While we primarily focussed on the SLE-associated *USP18* locus in our analysis, we have publicly released the complete genome-wide summary statistics from our MetaLCL project via the eQTL Catalogue FTP server. In addition to disease-specific colocalisation applications, we expect that our summary statistics will motivate the development and application of novel summary-based aggregative *trans*-eQTL mapping methods[59–61].

While the GWAS signal for SLE at the *USP18* locus was discovered in East Asian cohorts[33], our *trans*-eQTL analysis was based on samples of predominantly European genetic ancestry. The shared GWAS and *trans*-eQTL lead variant (rs4819670) is common in both genetic ancestry groups (EAS MAF = 0.16; EUR MAF = 0.36), indicating that allele frequency differences alone cannot explain why the SLE GWAS association has not been detected in European ancestry individuals. However, prevalence, severity and age of onset of SLE varies considerably between ancestry groups[62]. Furthermore, heterogeneity of GWAS effect sizes between European and

East Asian SLE GWAS studies has been reported[62]. Mechanisms of this genetic heterogeneity are unknown, but one plausible explanation is the presence of gene-environment interactions (e.g. diet or exposure to regional pathogens). In contrast, eQTL effect sizes in cultured LCLs are highly concordant between genetic ancestry groups[30], indicating that our use of European-ancestry samples to interpret a GWAS hit discovered in East Asians is unlikely to systematically bias our results in this case. Furthermore, the *USP18 trans*-eQTL signal replicated in a multi-ancestry cohort[30], indicating that the *trans*-eQTL effect is shared across ancestries.

Despite the strong evidence for the critical role of type I interferon response in SLE pathogenesis[43,44] and three active clinical trials, we were surprised to see that of the 50 USP18 target genes, only *OAS1* had an independent *cis*-association with SLE. Expanding the analysis to interferon response genes from Reactome further implicated IRF1/5/8 genes and the HLA region, but most interferon response genes were not detected in the SLE GWAS. One potential explanation for this could be the limited statistical power of the SLE GWAS that profiled 13,377 cases and 194,993 controls, identifying a total of 113 loci[33]. Furthermore, Liu *et al* demonstrated that if multiple effector genes ('core' genes) are co-regulated by shared *trans* factors, with shared directions of effects (which seems to be the case for the interferon response genes), then nearly all heritability would be due to *trans* effects, further reducing the power to detect *cis*-acting signals at individual target genes[4].

However, interferon response involves rapid upregulation of a broad transcriptional regulatory network of genes with diverse biological functions, only a subset of which might have a direct causal effect on SLE. This is supported by the fact that among the 38 interferon response genes (category II), only *OAS1*, *ADAR*, *PSMB8*, *SAMHD1* and the IRF transcription factors have been implicated in causing primary immunodeficiencies (Figure 3B). The remaining interferon response genes might thus be better thought of as biomarkers of the complex effect of interferon signalling on multiple parts of the immune system[44,63]. Similarly, it has been previously shown that variants in the *IL6R* region that are associated with circulating C-reactive protein (CRP) concentrations, are also associated with coronary artery disease (CAD) risk[64], but variants in the *CRP* region are not[65]. Thus, plasma levels of CRP do not seem to have a direct causal effect on CAD risk, but can still act as a molecular readout (biomarker) of the *IL6R*-mediated inflammatory response that does seem to have a causal effect[66]. These observations suggest that widespread horizontal pleiotropy in gene regulatory networks could be a general property of *trans*-QTLs and could help explain why using *trans*-pQTL signals in Mendelian randomisation analysis has had low specificity for identifying known drug targets[67,68]. Instead, we propose that target genes identified from large-scale *trans*-QTL studies could be better thought of as drug response biomarkers for drugs targeting the *cis* gene responsible for the *trans* association[8].

A limitation of our *trans*-eQTL analysis is its susceptibility to cross-mappability artefacts (Table S3). While heuristic approaches have been developed to filter such artefacts *post hoc*, these approaches are not guaranteed to remove all cross-mappability effects and might be too conservative at other loci[29]. Cross-mappability artefacts also tend to replicate well in independent cohorts[29]. Furthermore, as the sample size of *trans*-eQTL studies increases, the

power to detect subtle cross-mappability effects as putative *trans*-eQTLs also increases. To avoid these false positives, we used a very conservative strategy of requiring each *trans*-eQTL locus to have at least five independent target genes that all pass the cross-mappability filter. As a result, we likely missed many true *trans*-eQTLs regulating single or few target genes (e.g. *trans*-eQTL effect near the CIITA transcription factor on multiple HLA genes that has been replicated in several independent studies[6,31,69–71], Table S2). Future large-scale *trans*-eQTL studies will likely require the development of novel methods to properly adjust for cross-mappability, such as explicit modelling of transcript compatibility read counts between *cis* and trans *target* genes[72].

While large-scale *trans*-eQTL studies using both bulk and single-cell measurements are likely to continue for easily accessible tissues such as whole blood (e.g. eQTLGen Phase 2[73]), it seems unlikely that we will be able to perform *trans*-eQTL studies comprising tens of thousands of individuals for all disease-relevant cell types and contexts. A promising alternative is to use arrayed CRISPR screens or single-cell approaches to identify downstream gene-regulatory effects of disease-associated genes or individual genetic variants[40,74,75].

Methods

Datasets, samples and ethics

We used genotype and gene expression data from ALSPAC[31,76,77], TwinsUK[78], CoLaus[79,80], GEUVADIS[81], MRCA[82], MRCE[82], GENCORD[83], GTEx v8[17] and CAP[84] studies. For replication, we used data from the MAGE cohort[30]. The RNA sequencing and genotype data from the GEUVADIS and MAGE studies was publicly available as part of the 1000 Genomes project. For the other studies, we applied for access to individual-level data via relevant data access committees (DACs), explaining the aim of our project and the intent to publicly share meta-analysis summary statistics. Informed consent was obtained when research participants joined the ten studies listed above. The use of the CAP data for this project was approved by the National Heart, Lung and Blood Institute DAC. The use of the GTEx data for this project was approved by the National Human Genome Research Institute DAC. The use of the GENCORD data for this project was approved by the GENCORD DAC. The use of the MRCA and MRCE data for this project was approved by the Gabriel Consortium DAC. The use of TwinsUK data for this project was approved by the TwinsUK Resource Executive Committee. The use of the ALSPAC data for this project was approved by the ALSPAC Executive Committee. For the ALSPAC cohort, ethical approval for the study was obtained from the ALSPAC Ethics and Law Committee and the Local Research Ethics Committees. Consent for biological samples has been collected in accordance with the Human Tissue Act (2004). The CoLaus study was approved by the Institutional Ethics Committee of the University of Lausanne.
Single-cell RNA-seq samples were sourced ethically, and their research use was in accord with the terms of informed consent under an institutional review board/ethics committee-approved protocol (UK Regional Ethics Committee approval granted to work at Wellcome Sanger Institute, protocol reference number 15/NW/0282; project was approved by the Ethics on Research

390 Committee of the Institute of Neurobiology at Universidad Nacional Autonoma de Mexico
391 (UNAM), with the approval number 110.H.).

392 Genotype data quality control and imputation

393 **Pre-imputation quality control.** Genotype imputation was performed as described
394 previously[35]. Briefly, we lifted coordinates of the genotyped variants to the GRCh38 build with
395 CrossMap v0.4.1[85]. We aligned the strands of the genotyped variants to the 1000 Genomes 30x
396 on GRCh38 reference panel[86] using Genotype Harmonizer[87]. We excluded genetic variants with
397 Hardy-Weinberg p-value < 10^{-6}, missingness > 0.05 and minor allele frequency < 0.01 from
398 further analysis. We also excluded samples with more than 5% of their genotypes missing.
399
400 **Genotype imputation and quality control.** Most of the datasets were imputed using the 1000
401 Genomes reference panel based on the GRCh38 genome version. CoLaus dataset was
402 imputed using the TOPMed Imputation Server[88–90], while still aligning with the same reference
403 genome version. Additionally, GEUVADIS, GTEx and MAGE cohorts utilised whole genome
404 sequencing data aligned to the GRCh38 reference genome.
405
406 We pre-phased and imputed the microarray genotypes to the 1000 Genomes 30x on GRCh38
407 reference panel[86] using Eagle v2.4.1[91] and Minimac4[89]. We used bcftools v1.9.0 to exclude
408 variants with minor allele frequency (MAF) < 0.01 and imputation quality score R^2 < 0.4 from
409 downstream analysis. The genotype imputation and quality control steps are implemented in
410 eQTL-Catalogue/genimpute (v22.01.1) workflow available from GitHub. Subsequently, we used
411 QCTOOL v2.2.0 to convert imputed genotypes from VCF format to bgen format for *trans*-eQTL
412 analysis with regenie.

413 Gene expression data

414 **Studies**. We used gene expression data from seven RNA-seq studies (TwinsUK[78], CoLaus[79,80],
415 GEUVADIS[81], GENCORD[83], GTEx v8[17], CAP[84], MAGE[30]) and three microarray studies
416 (ALSPAC[31,76,77], MRCA[82] and MRCE[82]).
417
418 **RNA-seq quantification and normalisation**. RNA-seq data were pre-processed as described
419 previously[92]. Briefly, quantification of the RNA-seq data was performed using the eQTL-
420 Catalogue/rnaseq workflow (v22.05.1) implemented in Nextflow. Before quantification, we used
421 Trim Galore v0.5.0 to remove sequencing adapters from the fastq files. For gene expression
422 quantification, we used HISAT2[93] v2.2.1 to align reads to the GRCh38 reference genome
423 (Homo_sapiens.GRCh38.dna.primary_assembly.fa file downloaded from Ensembl). We counted
424 the number of reads overlapping the genes in the GENCODE V30 reference transcriptome
425 annotations with featureCounts v1.6.4.
426
427 We excluded all samples that failed the quality control steps as described previously[92]. We
428 normalised the gene counts using the conditional quantile normalisation (cqn) R package
429 v1.30.0 with gene GC nucleotide content as a covariate. We downloaded the gene GC content
430 estimates from Ensembl biomaRt and calculated the exon-level GC content using bedtools

431 v2.19.0[94]. We also excluded lowly expressed genes, where 95 per cent of the samples within a
432 dataset had transcripts per million (TPM)-normalised expression less than 1. Subsequently, we
433 used the inverse normal transformation to standardise quantification estimates. Normalisation
434 scripts together with containerised software are publicly available at https://github.com/eQTL-
435 Catalogue/qcnorm.
436
437 **Microarray data processing**. Gene expression from 877 individuals in the ALSPAC cohort was
438 profiled using Illumina Human HT-12 V3 BeadChips microarray. We used the normalised gene
439 expression matrix from the original publication[31]. In the MRCA cohort, gene expression from 327
440 individuals was profiled using the Human Genome U133 Plus 2.0 microarray. We downloaded
441 the raw CEL files from ArrayExpress (E-MTAB-1425) and normalised the data using the Robust
442 Multi-Array Average (RMA) method from the affy Bioconductor package[95]. In the MRCE cohort,
443 gene expression from 484 individuals was profiled using the Illumina Human-6 v1 Expression
444 BeadChip. As raw data was unavailable, we downloaded the processed gene expression matrix
445 from ArrayExpress (E-MTAB-1428). In all three microarray datasets, we applied inverse normal
446 transformation to each probe before performing *trans*-eQTL analysis. If there were multiple
447 probes mapping to the same gene, the probe with the highest average expression was used.

448 *Trans*-eQTL mapping and meta-analysis

449 We performed independent quality control and normalisation on all datasets and only included
450 18,792 protein coding genes in the analysis. *Trans*-eQTL analysis was conducted separately on
451 each dataset with regenie[96]. For studies containing related samples (TwinsUK, MRCA and
452 MRCE) and ALSPAC, both step 1 and step 2 commands were employed, while for other
453 datasets with a smaller number of unrelated samples (Table S1), regenie was run in the linear
454 regression mode (step 2 only). We used sex and six principal components of the normalised
455 gene expression matrix and six principal components of genotype data as covariates in the
456 *trans*-eQTL analysis. All scripts used to run *trans*-eQTL are publicly available at
457 https://github.com/freimannk/regenie_analysis. Subsequently, we performed an inverse-
458 variance weighted meta-analysis across studies. Meta-analysis workflow is available at
459 https://github.com/freimannk/regenie_metaanalyse.
460
461 We used a *cis* window of ± 5Mb to assign identified eQTLs into *cis* and *trans* eQTLs. To
462 determine significant loci, we excluded variants proximal (±1.5Mb) to the most highly associated
463 variant per gene. This approach allowed us to identify distinct and robust signals while
464 mitigating potential confounding effects from nearby variants. By applying these filters, we found
465 79 *trans*-eQTLs loci at a suggestive p-value threshold of $1x10^{-11}$.

466 Accounting for cross-mappability

467 A major source of false positives in *trans*-eQTL analysis is cross-mappability, whereby RNA-seq
468 reads from gene A erroneously align to gene B, leading to very strong apparent *trans*-eQTL
469 signals[11,29]. To exclude potential cross-mappability artefacts, we excluded all *trans*-eQTLs
470 where there was high cross-mappability (cross-mappability score from Saha *et al*[29] > 1) between
471 the *trans*-eQTL target gene and at least one protein coding gene in the *cis* region (±1.5Mb) of

472 the *trans* eQTL lead variant. Since some of the strongest cross-mappability artefacts affected
473 one or few target genes (Table S3), we further restricted our analysis to *trans*-eQTL loci that
474 had five or more target genes with $p < 5x10^{-8}$ and cross-mappability score < 1.

475 Replication of *trans*-eQTL associations

476 **MAGE.** Since we used somewhat arbitrary thresholds to define the initial set of 10 loci (lead p-
477 value $< 1x10^{-11}$, five or more targets with $p < 5x10^{-8}$), we sought to replicate our findings in an
478 independent Multi-ancestry Analysis of Gene Expression (MAGE)[30] cohort. MAGE consisted of
479 data from 731 lymphoblastoid cell lines from the 1000 Genomes project, 682 of which also had
480 whole genome sequencing data available. We used two strategies to assess replication. First,
481 we assessed if the lead variant-gene pair was nominally significant ($p < 0.05$) in the replication
482 dataset with concordant direction of effect. Based on this criterion, 7/10 loci replicated (Table
483 S2). Secondly, since all of our loci had multiple target genes, we used the pi1 statistic to
484 estimate the proportion of FDR < 5% target gene at each locus that had a non-null p-value in
485 the replication dataset[97]. We used the qvalue R package[98] to calculate pi1 = 1-qvalue(5% FDR
486 trans gene p-values)$pi0. For 3/10 loci, the proportion of non-null p-values was > 0.5 (Table
487 S2). Note that replication in an independent cohort does not help to reduce false positives due
488 to cross-mappability, as cross-mappability artefacts tend to be highly replicable[29].
489
490 **eQTLGen Consortium**. The eQTLGen Consortium is an initiative to investigate the genetic
491 architecture of blood gene expression and to understand the genetic basis of complex traits. We
492 used interim summary statistics from eQTLGen phase 2, wherein a genome-wide eQTL
493 analysis has been performed in 52 cohorts, representing 43,301 individuals.
494
495 All 52 cohorts performed cohort-specific analyses as outlined in the eQTLGen analysis
496 cookbook (https://eqtlgen.github.io/eqtlgen-web-site/eQTLGen-p2-cookbook.html). Genotype
497 quality control was performed according to standard bioinformatics practices and included
498 quality metric-based variant and sample filtering, removing related samples, ethnic outliers and
499 population outliers. Genotype data was converted to genome build hg38 if not done so already
500 and the autosomes were imputed using the 1000 Genomes 30x on GRCh38 reference panel[86]
501 (all ancestries) using the eQTLGen imputation pipeline (eQTLGen/eQTLGenImpute).
502
503 Like the genotype data, gene expression data was processed using the eQTLGen data QC
504 pipeline (eQTLGen/DataQC). For array-based datasets, we used the results from the empirical
505 probe mapping approach from our previous study[6] to connect the most suitable probe to each
506 gene which has previously been to show expression in the combined BIOS whole blood
507 expression dataset. Raw expression data was further normalized in accordance with the
508 expression platform used (quantile normalization for Illumina expression arrays and TMM[99] for
509 RNA-seq) and inverse normal transformation was performed. Gene expression outlier samples
510 were removed and gene summary information was collected for filtering at the central site.
511 Samples for whom there were mismatches in genetically inferred sex, reported sex, or the
512 expression of genes encoded from sex chromosomes were removed. Similarly, samples with
513 unclear sex, based on genetics or gene expression were removed.
514

515 An adaptation of the HASE framework[100] was used to perform genome-wide meta-analysis. For
516 genome-wide eQTLs analysis, this limits the data transfer size while ensuring participant
517 privacy. At each of the cohorts, the quality controlled and imputed data was processed and
518 encoded so that the individual level data can no longer be extracted, but while still allowing
519 effect sizes to be calculated for the linear relationship between variants and gene expression
520 (eQTLGen/ConvertVcf2Hdf5 and eQTLGen/PerCohortDataPreparations). Centrally, the meta-
521 analysis pipeline was run on the 52 cohorts. The pipeline which performs per cohort calculations
522 of effect sizes and standard errors and the inverse variance meta-analysis is available at
523 eQTLGen/MetaAnalysis. We included 4 genetic principal components, 20 gene expression
524 principal components and other technical covariates (e.g. RNA integrity number) where
525 available. Per every dataset, genes were included if the fraction of unique expression values
526 was equal or greater than 0.8, Variants were included based on imputation quality, Hardy-
527 Weinberg equilibrium (HWE) and minor allele frequency (MAF) (Mach R2 ≥ 0.4, HWE p ≥ 1×10-
528 6 and MAF ≥ 0.01). In an additional step, genes were filtered to include only those genes that
529 were available in at least 50% of the cohorts and 50% of the samples.

530 Differential gene expression in SLE cases *versus* controls

531 We re-analysed the microarray gene expression data from Banchereau et al. 2016[43] to explore
532 differential gene expression between SLE cases and controls. After downloading the processed
533 data from GEO (GSE65391), we selected one sample from each individual for our analysis
534 based on their earliest recorded visits. The filtered dataset comprised a total of 204 samples,
535 including 46 samples from healthy individuals and 158 samples from individuals diagnosed with
536 SLE. We also applied the inverse normal transformation to standardise the gene expression
537 values. Subsequently, we used the Python statsmodels[101] module to fit a linear model to identify
538 genes that were differentially expressed between SLE cases and controls. We included gender,
539 age and batch as covariates in all models.

540 Overlap between *USP18* target genes and GWAS hits for SLE

541 We download the list of prioritised target genes for the Yin *et al* GWAS study (GCST011956)
542 from the Open Targets Genetics Portal. We combined the list of genes prioritised by either the
543 L2G or the closest gene approach, yielding n = 109 target genes. We then overlapped these
544 target lists with the list of 50 *trans*-eQTL targets for the *USP18* locus (FDR < 5%).

545 Single-cell differential gene expression in resting and stimulated B-cells

546 **Sample collection, cell isolation and cryopreservation**. Blood samples were collected from
547 five healthy Mexican individuals (three males and two females). Peripheral blood mononuclear
548 cells (PBMCs) were isolated using Vacutainer CPT tubes, according to manufacturer
549 instructions. Samples were cryopreserved in RPMI 1640 culture media (Sigma), Fetal Bovine
550 Serum (FBS) and Dimethyl sulfoxide (DMSO) and stored at -80ºC for 24h, before being
551 transferred to liquid nitrogen.
552

553 **Thawing and stimulation.** Cryopreserved PBMCs were thawed quickly and washed in 14mL of
554 room temperature complete RPMI 1640 media (10% FBS, 1% Penicillin-Streptomycin, 1% L-
555 Glutamine). Cells were incubated at 37 °C, 5% CO_2 for 2h. Cells were then stimulated with
556 interferon alpha (IFN-α, Bio-techne) and R-848 (Resiquimod, Cambridge Bioscience) at a
557 working concentration of 1000U/mL and 2μg/ml, respectively. Cells were incubated at 37 °C, 5%
558 CO2 and harvested after 16h, 40h and 64h of stimulation. Unstimulated cells were kept in
559 culture without any stimuli for 16h (i.e., 0h of activation).
560
561 **Multiplexing, CITE-seq staining & scRNA-seq**. Upon harvesting, cells were resuspended in a
562 cell staining buffer (Biolegend) and cell hashing and genotype-based multiplexing was
563 performed. Donors of the same stimulation condition were mixed at equal ratios (each pool
564 corresponded to a mix of cells from four to five different individuals). These pools were stained
565 with the TotalSeq-C Human Universal Cocktail, V1.0 (137 cell surface proteins (CSP),
566 Biolegend), in addition to a unique hashtag antibody oligonucleotide (HTO, Biolegend) which
567 corresponds to the stimulation condition pool. After staining and washing, all stimuli condition
568 pools were pooled together at equal ratios. This pool was then stained with live/dead dye 4,6-
569 diamidino-2-phenylindole (DAPI, Biolegend) and dead cells were removed using fluorescence-
570 activated cell sorting.
571
572 Cells were next processed using the 10X Genomics Immune Profiling 5' high-throughput (HT)
573 v2 kit, as specified by the manufacturer's instructions. $1.15x10^5$ cells were loaded into each inlet
574 of a 10X Chromium X to create Gel Bead-in-emulsions (GEMs). Two 10X HT reactions were
575 loaded per time point of sample processing (targeted recovery was 40,000 cells per 10X
576 reaction). Reverse transcription was performed on the emulsion, after which cDNA and CITEseq
577 supernatant were purified, amplified and used to construct RNA-sequencing and CSP
578 sequencing libraries, respectively. These RNA and CSP libraries were sequenced at a 5:1 ratio,
579 respectively, using the Illumina NoveSeq 6000 S4, with 100-bp paired-end reads and all 10X
580 reactions were mixed at equal ratios and sequenced across two lanes.
581
582 **Deconvolution of single cells by genotype**. Each 10X reaction comprised a mix of cells from
583 unrelated individuals. Thus, natural genetic variation was used to assign cells to their respective
584 individuals. First, a list of common exonic variants was compiled from the 1000 Genomes
585 Project phase 3 exome-sequencing data (MAF> 0.05). Next, cellSNP (v1.2.1) was used to
586 generate pileups at the genomic location of these variants. These pileups, in combination with
587 the variants called from genotyping in each individual, were used as an input for Vireo[102]
588 (v0.5.7). If any cell had less than 0.9 posterior probability of belonging to any individual or were
589 of mixed genotypes they were labelled as 'unassigned' and 'doublets', respectively, and
590 removed from downstream analysis.
591
592 **Data processing and quality controls**. Raw scRNA-seq and CITE-seq data were processed
593 using the Cell Ranger Multi pipeline (v7.0.0, 10x Genomics). In brief, RNA and CSP library
594 reads were first assigned to cells. RNA reads were then aligned to the GRCh38 human
595 reference genome and CSP antibody reads were matched to the provided list of known
596 barcodes. Ensembl version 93 was used as a reference for gene annotation, and gene

expression was quantified using reads assigned to cells and confidently mapped to the genome. Additionally, Cell Ranger multi was used to deconvolute samples based on HTOs. It uses an algorithm which employs a latent variable model over a state space composed of each HTO used in the experiment to assign each cell to a stimulation condition or as a doublet.

Results from RNA and CSP quantification in Cell Ranger were imported into RStudio (v4.3.1) and analysed using Seurat (v5.0.1). Any cell identified as doublet or unassigned by Vireo and or antibody hashtag deconvolution method were excluded. 10X reactions were split by time point and stimuli condition. Cells with 1.5 - 2.5 median absolute deviations below the median of genes and counts detected were discarded. Additionally, cells with 3 - 4 median absolute deviation above the median for the percentage of mitochondrial reads detected were discarded. The resulting cells were then annotated by Azimuth[103] (v0.5.0), using the Azimuth PBMC reference dataset that was generated as part of the Hao and Hao *et al*, 2021 paper[103].

Pseudobulk and normalisation. Raw counts were pseudobulked by Azimuth annotated level 1 cell types (CD4, CD8, B, Mono, DC, NK, Other and Other T) per donor, per time point and per stimulation condition, via edgeR[104] (v4.0.16). Pseudobulked raw counts were then counts per million (CPM) normalised and $\log_2$ transformed with edgeR.

Data availability

The whole genome sequencing data for the GEUVADIS and MAGE studies was downloaded from the 1000 Genomes website. The GEUVADIS RNA-seq data was downloaded from the European Nucleotide Archive (ENA) under accession PRJEB3366. The MAGE RNA-seq data was downloaded from the ENA (accession PRJNA851328). The genotype and RNA-seq data from the GENCORD study was downloaded from European Genotype-phenotype Archive (EGA) under accessions EGAD00001000425 and EGAD00001000428. The microarray gene expression data from the MRCA and MRCE studies was downloaded from ArrayExpress (E-MTAB-1425 and E-MTAB-1428) and the genotype data was downloaded from EGA (EGAS00000000137). The gene expression and genotype data from GTEx and CAP studies was downloaded from dbGaP (accessions phs000424.v8.p2 and phs000481.v3.p2). The RNA-seq data from the TwinsUK study was downloaded from EGA (EGAD00001001086) and genotype data was obtained from TwinsUK (https://twinsuk.ac.uk/resources-for-researchers/access-our-data/). The informed consent obtained from ALSPAC participants does not allow the microarray and genotype data to be made freely available through any third party maintained public repository. However, data used for this study can be made available on request to the ALSPAC Executive. The ALSPAC data management plan describes in detail the policy regarding data sharing, which is through a system of managed open access. Full instructions for applying for data access can be found here: http://www.bristol.ac.uk/alspac/researchers/access/. The ALSPAC study website contains details of all the data that are available (http://www.bristol.ac.uk/alspac/researchers/our-data/). The RNA-seq and genotype data from the CoLaus cohort can be accessed by directly contacting the cohort (https://www.colaus-psycolaus.ch/professionals/how-to-collaborate/). The

MetaLCL full *trans*-eQTL meta-analysis summary statistics are available from the eQTL Catalogue FTP server (https://www.ebi.ac.uk/eqtl/Data_access/) and additional documentation is available on the project website (https://github.com/AlasooLab/MetaLCL).

URLs

MetaLCL website: https://github.com/AlasooLab/MetaLCL
MetaLCL t*rans*-eQTL analysis workflow: https://github.com/freimannk/regenie_analysis
MetaLCL meta-analysis workflow: https://github.com/freimannk/regenie_metaanalyse
eQTL Catalogue website: https://www.ebi.ac.uk/eqtl/Data_access/
eQTL Catalogue genotype imputation workflow: https://github.com/eQTL-Catalogue/genimpute
eQTL Catalogue RNA-seq processing workflow: https://github.com/eQTL-Catalogue/rnaseq
eQTL Catalogue data normalisation workflow: https://github.com/eQTL-Catalogue/qcnorm
eQTLGen analysis cookbook: https://eqtlgen.github.io/eqtlgen-web-site/eQTLGen-p2-cookbook.html
eQTLGen data QC workflow: https://github.com/eQTLGen/DataQC
eQTLGen genotype conversion workflow: https://github.com/eQTLGen/ConvertVcf2Hdf5
eQTLGen per-cohort analysis workflow: https://github.com/eQTLGen/PerCohortDataPreparations
eQTLGen meta-analysis workflow: https://github.com/eQTLGen/MetaAnalysis
eQTLGen genotype imputation workflow: https://github.com/eQTLGen/eQTLGenImpute
QCTOOL: https://www.chg.ox.ac.uk/~gav/qctool_v2/

Declaration of interests

The authors declare no competing interests.

Acknowledgements

Most of the analysis presented in the paper were performed at the High Performance Computing Center, University of Tartu. We are extremely grateful to all the families who took part in the ALSPAC study, the midwives for their help in recruiting them, and the whole ALSPAC team, which includes interviewers, computer and laboratory technicians, clerical workers, research scientists, volunteers, managers, receptionists and nurses. This work received support from Christian Molina-Aguilar, Carina Uribe Díaz, and Alejandra Castillo Carbajal. We thank the FACS facility and sequencing pipelines at Wellcome Sanger Institute for their assistance in data generation, and the Human Genetics Informatics for their support in sequence data processing. We thank Bess L. Chau for assistance in the experiments involving generation of single-cell RNAseq data from stimulated PBMCs. We thank Karatug Ozan Bircan, Abayomi Mosaku, Laura Harris and Helen Parkinson for assistance with hosting the full *trans*-eQTL summary statistics on the eQTL Catalogue FTP server.

Funding

K.F and L.S. were supported by a grant from Open Targets (grant no. OTAR2069). K.A was supported by the Estonian Research Council (grant no. PSG415). K.A. also received funding from the European Union's Horizon 2020 research and innovation program (grant no. 825775). GT, CPJ and TSR were supported by Open Targets (grant no. OTAR2064) and the Wellcome Grant (ref. 220540/Z/20/A, 'Wellcome Sanger Institute Quinquennial Review 2021-2026). SB was supported by the Swiss National Science Foundation (grant no. 310030_152724/1). K.K. was supported by the Estonian Research Council (grant no. PRG1117). AMR was supported by CONACYT-FORDECYT-PRONACES grant no. [11311] and Programa de Apoyo a Proyectos de Investigación e Innovación Tecnológica–Universidad Nacional Autónoma de México (PAPIIT-UNAM) IN218023. ALHL is a doctoral student from Programa de Doctorado en Ciencias Biomédicas, Universidad Nacional Autónoma de México (UNAM), and she receives fellowship 790972 from Consejo Nacional de Humanidades, Ciencias y Tecnologías CONAHCYT, México. The UK Medical Research Council and Wellcome (Grant ref: 217065/Z/19/Z) and the University of Bristol provide core support for ALSPAC. ALSPAC GWAS data was generated by Sample Logistics and Genotyping Facilities at Wellcome Sanger Institute and LabCorp (Laboratory Corporation of America) using support from 23andMe. This publication is the work of the authors and they will serve as guarantors for the contents of this paper.

Author contributions

K.F. performed *trans*-eQTL analysis on nine cohorts and also performed the meta-analysis across cohorts. A.B. performed *trans*-eQTL analysis on the CoLaus cohort. K.F., J.C., E.R.H., J.C.M., N.N., H.O., L.S., M.C.T., G.T., K.K. and K.A. interpreted the results and prioritised follow-up analyses. T.S.R. generated and analysed single-cell RNAseq data under C.P.J. and G.T. supervision. A.L.H.-L. collected blood samples for single-cell RNAseq under A.M.-R. supervision. R.W. performed replications in the eQTLGen Consortium under U.V. and L.F. supervision. S.B. and K.A. supervised the research. K.F. and K.A. wrote the manuscript with feedback from all authors.

Supplementary Information

1. eQTLGen Consortium - Author information
2. Supplementary Note
3. Table S1
4. Figure S1-S9

eQTLGen Consortium – Author information

Author list is ordered alphabetically.

Habibul Ahsan[1], Marta E. Alarcón-Riquelme[2,3], Philip Awadalla[4], Guillermo Barturen[5,6,2], Alexis Battle[7], Frank Beutner[8], Cornelis Blauwendraat[9,10], Collins Boahen[11,12], Toni Boltz[13], Dorret I. Boomsma[14,15,16], Andrew Brown[17], John Budde[18,19], Katie L. Burnham[20], John Chambers[21,22,23], Evans Cheruiyot[24], Surya B. Chhetri[25], Annique Claringbould[26,27], PRECISESADS Clinical Consortium[2], DIRECT Consortium[28], Carlos Cruchaga[18,29,30,31,32,33], Kensuke Daida[9,10,34], Emma E. Davenport[20], Devin Dikec[18,19], Théo Dupuis[17], Diptavo Dutta[35], Tõnu Esko[36], Radi Farhad[37], Aiman Farzeen[38,39], Marie-Julie Favé[40], Lude Franke[26,41], Tim Frayling[42], Koichi Fukunaga[43], J. Raphael Gibbs[44], Greg Gibson[45], Priyanka Gorijala[18,19], Binisha Hamal Mishra[46,47,48], Takanori Hasegawa[49], Michael Inouye[50,51,52,53,54,55], Farzana Jasmine[1], Matt Johnson[18,19], Muhammad G. Kibriya[1], Holger Kirsten[56,57], Julian C. Knight[58], Peter Kovacs[59,60], Knut Krohn[61], Viktorija Kukushkina[36], Vinod Kumar[11,12,62,63], Mika Kähönen[47,64], Sandra Lapinska[65], Terho Lehtimäki[46,47,48], Yun Li[66,67,68], Markus Loeffler[69,70], Marie Loh[21,71,72,23], Leo-Pekka Lyytikäinen[46,47,48], Javier Martin[73], Angel Martinez-Perez[74], Allan McRae[24], Lili Milani[36], Pashupati P. Mishra[46,47,48], Younes Mokrab[37], Grant Montgomery[24], Juha Mykkänen[75,76], Reedik Mägi[36], Martina Müller-Nurasyid[77], Haroon Naeem[37], Sini Nagpal[45], Ho Namkoong[78], Matthias Nauck[79], Yukinori Okada[80,81,82,83,84], Roel Ophoff[65,13,85], Katja Pahkala[76,75,86], Bogdan Pasaniuc[65,87,13,88], Dirk S. Paul[50,51,89], Elodie Persyn[50,51,90], Brandon Pierce[1], René Pool[91,15], Holger Prokisch[92,93], Laura Raffield[67], Venket Raghavan[69], Olli Raitakari[94,95,75,96], Emma Raitoharju[97,98], Jansen Rick[15,99], María Rivas-Torrubia[2], Ruth D. Rodríguez[2], Suvi P. Rovio[76,75], Jessie Sanford[18,19], Markus Scholz[69,70], Eline Slagboom[100], José Manuel Soria[74], Juan Carlos Souto[74], Michael Stumvoll[101,102,103], Yun Ju Sung[18,19], Darwin Tay[21], Alexander Teumer[104,105], Joachim Thiery[70,106], Alex Tokolyi[20], Lin Tong[1], Anke Tönjes[101], Jan Veldink[107], Joost Verlouw[108], Peter M. Visscher[24], Ana Viñuela[109], Urmo Võsa[36], Uwe Völker[110,111], Qingbo S. Wang[80,81,82], Robert Warmerdam[26,41], Stefan Weiss[112,113], Jia Wen[67], Harm-Jan Westra[26,41], Andrew Wood[42], Manke Xie[45], Dasha Zhernakova[26], Marleen van Greevenbroek[114], Joyce van Meurs[115,116]

1. Department of Public Health Sciences, University of Chicago, Illinois, USA
2. Pfizer–University of Granada–Junta de Andalucía Centre for Genomics and Oncological Research, Granada, Spain
3. Institute of Environmental Medicine, Karolinska Institute, Stockholm, Sweden
4. Ontario Institute for Cancer Research, University of Toronto
5. Department of Genetics, Faculty of Science, University of Granada, 18071 Granada, Spain
6. Bioinformatics Laboratory, Biotechnology Institute, Centro de Investigación Biomédica, PTS, Avda. del Conocimiento s/n, 18100 Granada, Spain
7. Department of Biomedical Engineering, Department of Computer Science, Department of Genetic Medicine, Johns Hopkins University, Baltimore, MD, USA
8. Department of Internal Medicine/Cardiology, Heart Center Leipzig at Leipzig University, Leipzig, Germany
9. Integrative Neurogenomics Unit, Laboratory of Neurogenetics, National Institute on Aging, National Institutes of Health, Bethesda, MD, USA
10. Center for Alzheimer's and Related Dementias (CARD), National Institute on Aging and National Institute of Neurological Disorders and Stroke, National Institutes of Health, Bethesda, MD, USA
11. Department of Internal Medicine and Radboud Institute of Molecular Life Sciences (RIMLS), Radboud University Medical Center, Nijmegen, 6525 HP, the Netherlands

12. Department of Internal Medicine and Radboud Center for Infectious Diseases (RCI), Radboud University Medical Center, Nijmegen, 6525 HP, the Netherlands
13. Department of Human Genetics, David Geffen School of Medicine, University of California Los Angeles, Los Angeles, CA, USA
14. Amsterdam Reproduction & Development (AR&D) research institute, Amsterdam, the Netherlands
15. Amsterdam Public Health research institute, Amsterdam, the Netherlands
16. Department of Complex Trait Genetics, Center for Neurogenomics and Cognitive Research, Amsterdam, Vrije Universiteit Amsterdam
17. Population Health and Genomics, University of Dundee, Dundee, Scotland, UK.
18. Department of Psychiatry, Washington University School of Medicine, St. Louis, MO, United States
19. NeuroGenomics and Informatics Center, Washington University School of Medicine, St. Louis, MO 63110, USA
20. Wellcome Sanger Institute, Wellcome Genome Campus, Hinxton, UK
21. Lee Kong Chian School of Medicine, Nanyang Technological University, Singapore
22. Precision Health Research (PRECISE), Singapore
23. Department of Epidemiology and Biostatistics, School of Public Health, Imperial College London, United Kingdom
24. Institute for Molecular Bioscience, The University of Queensland, Brisbane, QLD, 4072, Australia
25. Department of Biomedical Engineering, Johns Hopkins University, Baltimore, MD, USA
26. Department of Genetics, University Medical Center Groningen, University of Groningen, Groningen, The Netherlands
27. Department of Internal Medicine, Erasmus MC, Erasmus University Medical Center Rotterdam, Rotterdam, The Netherlands
28. https://directdiabetes.org/
29. NeuroGenomics and Informatics Center, Washington University School of Medicine, St. Louis, MO 63110, USA
30. Department of Neurology, Washington University School of Medicine, St. Louis, MO 63110, USA
31. Knight Alzheimer Disease Research Center, Washington University School of Medicine, St. Louis, MO, United States
32. Hope Center for Neurological Disorders, Washington University School of Medicine, St. Louis, MO, United States
33. Dominantly Inherited Alzheimer Disease Network (DIAN)
34. Department of Neurology, Faculty of Medicine, Juntendo University, Tokyo, Japan
35. Division of Cancer Epidemiology & Genetics, National Cancer Insititute, Bethesda, MD, USA
36. Estonian Genome Centre, Institute of Genomics, University of Tartu, Tartu, Estonia
37. Human Genetics Department, Sidra Medicine, Doha, Qatar
38. Institute of Human Genetics, School of Medicine, Technische Universität München, Munich, Germany
39. Institute of Neurogenomics, Computational Health Center, Helmholtz Zentrum München, Munich, Germany.
40. Ontario Institute for Cancer Research
41. Oncode Institute, Groningen, The Netherlands
42. Genetics of Complex Traits, University of Exeter Medical School, Exeter, UK
43. Division of Pulmonary Medicine, Department of Medicine, Keio University School of Medicine, Tokyo, Japan.
44. Computational Biology Group, Laboratory of Neurogenetics, National Institute on Aging, Bethesda, MD, USA
45. Center for Integrative Genomics, Georgia Institute of Technology, Atlanta, GA, USA.
46. Department of Clinical Chemistry, Faculty of Medicine and Health Technology, Tampere University, Tampere, Finland

47. Finnish Cardiovascular Research Center Tampere, Faculty of Medicine and Health Technology, Tampere University, Tampere, Finland
48. Department of Clinical Chemistry, Fimlab Laboratories, Tampere, Finland
49. M&D Data Science Center, Tokyo Medical and Dental University, Tokyo, Japan.
50. British Heart Foundation Cardiovascular Epidemiology Unit, Department of Public Health and Primary Care, University of Cambridge, Cambridge, UK
51. Victor Phillip Dahdaleh Heart and Lung Research Institute, University of Cambridge, Cambridge, UK
52. Cambridge Baker Systems Genomics Initiative, Department of Public Health and Primary Care, University of Cambridge, Cambridge, UK
53. Cambridge Baker Systems Genomics Initiative, Baker Heart and Diabetes Institute, Melbourne, VIC, Australia
54. Health Data Research UK Cambridge, Wellcome Genome Campus and University of Cambridge, Cambridge, UK
55. British Heart Foundation Centre of Research Excellence, University of Cambridge, Cambridge, UK.
56. LIFE – Leipzig Research Center for Civilization Diseases, Leipzig University, Germany
57. Institute for Medical Informatics, Statistics and Epidemiology, Leipzig University, Germany
58. Centre for Human Genetics, University of Oxford, Oxford, UK
59. Integrated Research and Treatment Center (IFB) Adiposity Diseases, University of Leipzig, D-04103 Leipzig, Germany
60. Department of Medicine, University of Leipzig, D-04103 Leipzig, Germany
61. Medical Faculty, University of Leipzig, Leipzig, Germany.
62. Department of Genetics, University of Groningen, University Medical Center Groningen, Groningen, 9700 RB, the Netherlands
63. Nitte (Deemed to Be University), Medical Sciences Complex, Nitte University Centre for Science Education and Research (NUCSER), Deralakatte, Mangalore, 575018, India
64. Department of Clinical Physiology, Tampere University Hospital, Tampere Finland
65. Bioinformatics Interdepartmental Program, University of California Los Angeles, Los Angeles, CA, USA
66. Department of Biostatistics, University of North Carolina at Chapel Hill, Chapel Hill, NC, USA
67. Department of Genetics, University of North Carolina, Chapel Hill, NC, USA
68. Department of Computer Science, University of North Carolina at Chapel Hill, Chapel Hill, NC, USA
69. Institute for Medical Informatics, Statistics and Epidemiology, Leipzig University, Leipzig, Germany
70. Leipzig Research Centre for Civilization Diseases, Leipzig University, Leipzig, Germany
71. National Skin Centre, Research Division, Singapore
72. Genome Institute of Singapore, Agency for Science, Technology and Research, Singapore
73. Instituto de Parasitología y Biomedicina López-Neyra, Consejo Superior de Investigaciones Científicas (IPBLN-CSIC), Granada, Spain
74. Unit of Genomic of Complex Diseases, Institut de Recerca Sant Pau (IR Sant Pau), Barcelona, Spain.
75. Centre for Population Health Research, University of Turku and Turku University Hospital, Turku, Finland
76. Research Centre of Applied and Preventive Cardiovascular Medicine, University of Turku, Turku, Finland
77. Institute for Medical Biometry, Epidemiology and Informatics (IMBEI), Mainz, Germany
78. Department of Infectious Diseases, Keio University School of Medicine, Tokyo, Japan.
79. Institute of Clinical Chemistry and Laboratory Medicine, University Medicine Greifswald, Greifswald, Germany
80. Department of Genome Informatics, Graduate School of Medicine, the University of Tokyo, Tokyo, Japan
81. Department of Statistical Genetics, Osaka University Graduate School of Medicine, Suita, Japan

853 82. Laboratory for Systems Genetics, RIKEN Center for Integrative Medical Sciences, Yokohama, Japan
854 83. Laboratory of Statistical Immunology, Immunology Frontier Research Center (WPI-IFReC), Osaka
855 University, Suita, Japan
856 84. Premium Research Institute for Human Metaverse Medicine (WPI-PRIMe), Osaka University, Suita,
857 Japan.
858 85. Center for Neurobehavioral Genetics, Semel Institute for Neuroscience and Human Behavior, David
859 Geffen School of Medicine, University of California Los Angeles, Los Angeles, USA
860 86. Paavo Nurmi Centre, Unit of Health and Physical Activity, University of Turku, Turku, Finland
861 87. Department of Computational Medicine, David Geffen School of Medicine, University of California Los
862 Angeles, Los Angeles, CA, USA
863 88. Department of Pathology and Laboratory Medicine, David Geffen School of Medicine, University of
864 California Los Angeles, Los Angeles, CA, USA
865 89. Centre for Genomics Research, Discovery Sciences, BioPharmaceuticals R&D, AstraZeneca,
866 Cambridge, UK.
867 90. Cambridge Baker Systems Genomics Initiative, Department of Public Health and Primary Care,
868 University of Cambridge, UK.
869 91. Department of Biological Psychology, Vrije Universiteit Amsterdam, Amsterdam, the Netherlands
870 92. Institute of Neurogenomics, Computational Health Center, Helmholtz Zentrum München, Neuherberg,
871 Germany
872 93. School of Medicine, Institute of Human Genetics, Technical University of Munich, Munich, Germany
873 94. Research centre of Applied and Preventive Cardiovascular Medicine, University of Turku, Turku,
874 Finland
875 95. Department of Clinical Physiology and Nuclear Medicine, Turku University Hospital, Turku, Finland
876 96. InFLAMES Research Flagship, University of Turku, Turku, Finland
877 97. Molecular Epidemiology, Faculty of Medicine and Health Technology, Tampere University, Tampere,
878 Finland
879 98. Tampere University Hospital, Tampere, Finland
880 99. Amsterdam UMC location Vrije Universiteit Amsterdam, Department of Psychiatry & Amsterdam
881 Neuroscience -Complex Trait Genetics (VUmc) and Mood, Anxiety, Psychosis, Stress & Sleep
882 100. Section of Molecular Epidemiology, Department of Biomedical Data Sciences, Leiden University
883 Medical Center, Leiden, the Netherlands
884 101. Medical Department III-Endocrinology, Nephrology, Rheumatology, University of Leipzig Medical
885 Center, Leipzig, Germany
886 102. Helmholtz Institute for Metabolic, Obesity and Vascular Research (HI-MAG), Helmholtz Zentrum
887 München, University of Leipzig and University Hospital Leipzig, Leipzig, Germany
888 103. Deutsches Zentrum für Diabetesforschung, Neuherberg, Germany
889 104. Department of Psychiatry and Psychotherapy, University Medicine Greifswald, Greifswald, Germany
890 105. DZHK (German Center for Cardiovascular Research), partner site Greifswald, Greifswald, Germany
891 106. Institute of Laboratory Medicine, Clinical Chemistry and Molecular Diagnostics, University of Leipzig
892 Medical Center, Leipzig, Germany
893 107. Department of Neurology, UMC Utrecht Brain Center Rudolf Magnus, Utrecht, The Netherlands
894 108. Department of Internal Medicine, Erasmus University Medical Center, Rotterdam, The Netherlands
895 109. Biosciences Institute, Faculty of Medical Sciences, University of Newcastle, Newcastle upon Tyne,
896 UK
897 110. German Centre for Cardiovascular Research (DZHK), Partner Site Greifswald, D-17475 Greifswald,
898 Germany
899 111. Interfaculty Institute for Genetics and Functional Genomics, University Medicine Greifswald, Felix-
900 Hausdorff-Strasse 8, D-17475 Greifswald, Germany

901 112. Interfaculty Institute of Genetics and Functional Genomics, University Medicine Greifswald,
902 Greifswald, 17475, Germany
903 113. German Center for Cardiovascular Research (DZHK), Partner Site Greifswald, Greifswald, 17475,
904 Germany.
905 114. CARIM, Maastricht University
906 115. Department of Internal Medicine, Erasmus MC University Medical Center, Rotterdam, The
907 Netherlands
908 116. Department of Orthopaedics and Sportsmedicine, Erasmus MC University Medical Center,
909 Rotterdam, The Netherlands.

910

Supplementary Note

MYBL2 regulates the expression of many cell cycle genes

At the *MYBL2* locus, the lead variant chr20_43721344_C_T was associated with the expression of 151 target genes at FDR 5% (Figure S8). The target genes were strongly enriched for the Gene Ontology mitotic cell cycle term (GO:0000278, $p=2.607\times10^{-51}$) and the Reactome mitotic cell cycle pathway (R-HSA-69278, $p=1.216\times10^{-35}$). Interestingly, 125/151 genes (82%) had lower expression in carriers of the alternative T allele (Figure S8). The T allele of chr20_43721344_C_T was also strongly associated ($p =8.83x10^{-218}$) with the decreased expression of the *MYBL2* transcription factor gene in *cis (*Figure S8). Since both the MYBL2 transcription factor located in *cis* and majority of the *trans*-genes had lower expression in the carriers of the T allele, we hypothesised that MYBL2 might directly regulate these target genes. To test this, we download ChIP-seq data for the MYBL2 transcription factor in the human K562 myelogenous leukemia cell line from the ENCODE project (ENCSR162IEM). We then asked how many of the up- and downregulated genes had a MYBL2 ChIP-seq peak within +/- 2kb from the annotated promoter of the gene. We found that 99/125 (78.4%) downregulated genes had a MYBL2 peak in their promoter region (Figure S9). In contrast, only 1/26 upregulated genes had a MYBL2 peak in their promoter region. As a negative control, we looked at the 404 5% FDR target genes of the *SP140* locus (Table S2) and found that only 23/404 (5.6%) of the target genes had a MYBL2 peak in their promoter region (Figure S9).

To further understand which cell cycle stage these *MYBL2* target genes might be involved in, we obtained the list of genes specific to G2M and S phases of the cell cycle from Tirosh et al. 2015[105] using Seurat R package[106]. We found that 33/125 genes downregulated by the *trans*-eQTL variant were markers of the G2M phase which was significantly more than expected ($p = 1.23x10^{-53}$). In contrast, only 1/125 downregulated genes overlapped with markers of the S phase ($p = 0.36$). Of note, 2/26 upregulated genes overlapped S-phase markers ($p = 0.004$) and none of the upregulated genes overlapped G2M-phase markers.

Altogether, this evidence strongly suggests that MYBL2 directly regulates the expression of G2M genes in *trans* by binding to their promoter sequences and is directly involved in the regulation of the expression of these target genes.

943 **Table S1**. **Overview of the LCL eQTL discovery cohorts.** The cohorts included in the analysis
944 used a mixture of RNA-seq and microarray technologies and three cohorts (TwinsUK, MRCE

Cohort	Sample size	Expression data	Genotype data	Relatedness
ALSPAC[31,76,77]	877	microarray	imputed (1000G 30x on GRCh38)	unrelated
TwinsUK[78]	735	RNA-seq	imputed (1000G 30x on GRCh38)	twins
CoLaus[79,80]	553	RNA-seq	imputed (TOPMed)	unrelated
GEUVADIS[81]	358	RNA-seq	WGS (1000G 30x on GRCh38)	unrelated
Liang_2013 (MRCE)[82]	484	microarray	imputed (1000G 30x on GRCh38)	siblings
Liang_2013 (MRCA)[82]	327	microarray	imputed (1000G 30x on GRCh38)	siblings
GENCORD[83]	187	RNA-seq	imputed (1000G 30x on GRCh38)	unrelated
GTEx[17]	113	RNA-seq	WGS (GRCh38)	unrelated
CAP[84]	100	RNA-seq	imputed (1000G 30x on GRCh38)	unrelated
MAGE[30] (replication)	682	RNA-seq	WGS (GRCh38)	unrelated, diverse ancestries

945 and MRCA) contained related samples.
946

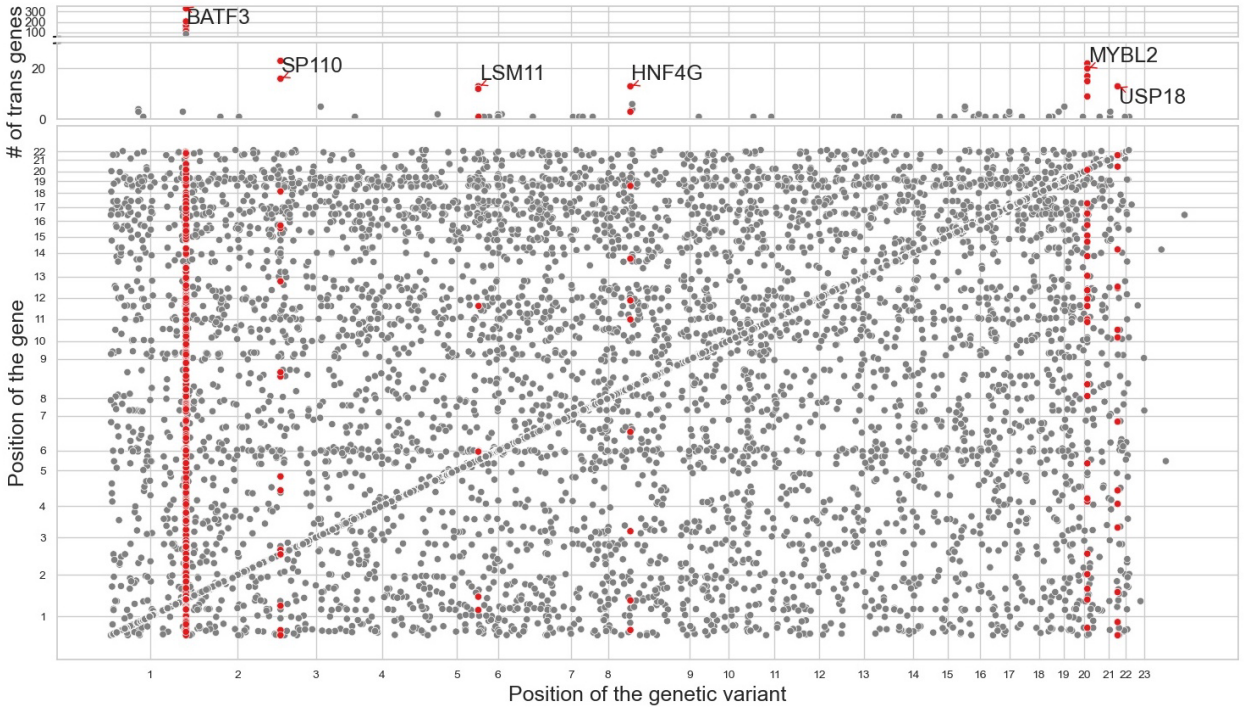

Figure S1. Overview of *trans*-eQTL results at the relaxed $p < 5x10^{-8}$ threshold. The upper scatter plot shows the number of *trans* associations detected at each *trans*-eQTL locus with p-values $< 5x10^{-8}$. Six largest *trans*-eQTL loci have been labelled with the name of the closest *cis* gene. The lower scatter plot shows all significant loci for each tested gene at the $p < 5x10^{-8}$ threshold. *Cis* associations are located on the diagonal while putative *trans* associations are located off diagonal.

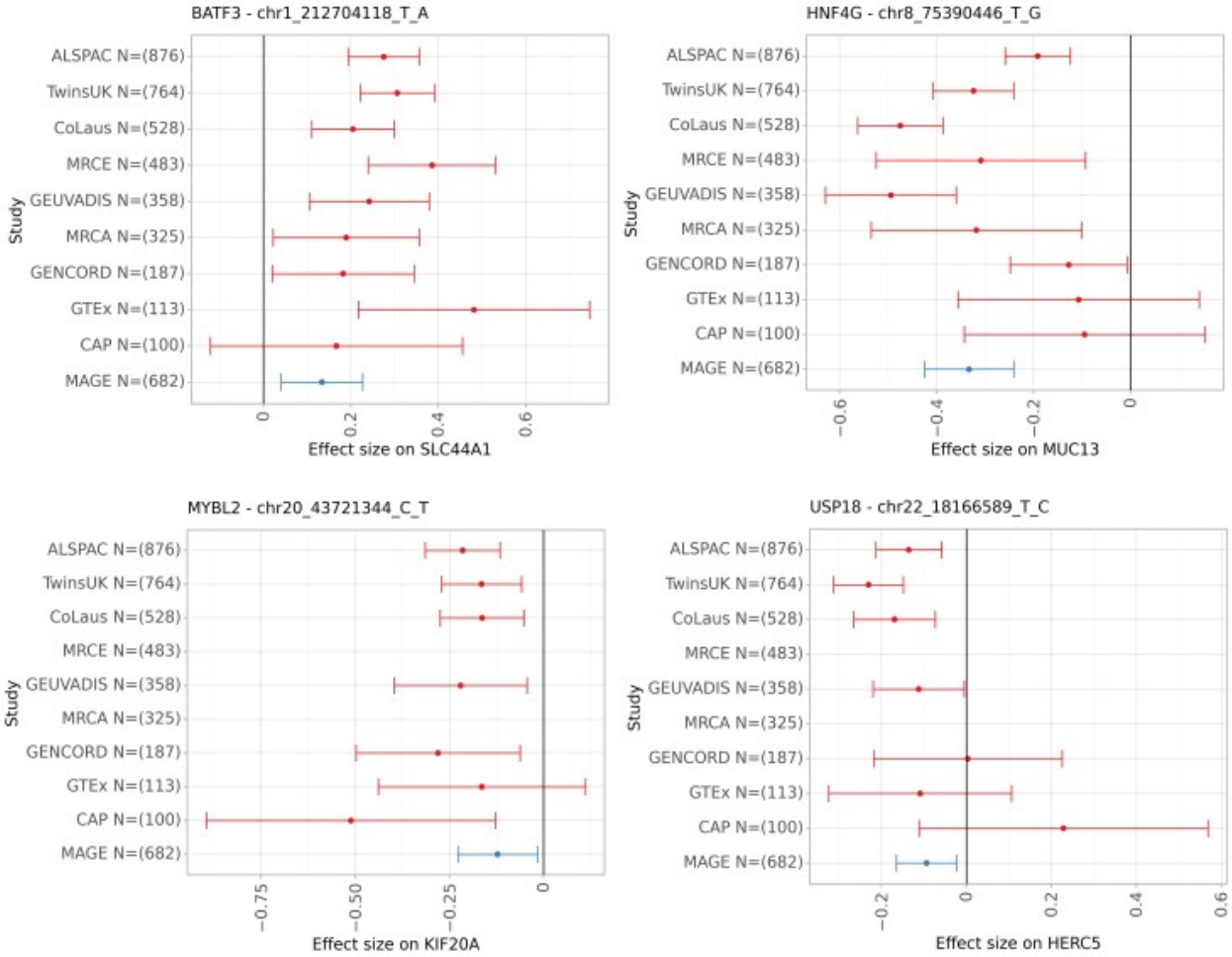

Figure S2. **Forest plots showing cohort-specific effect size for the four *trans*-eQTL loci that replicated in the MAGE cohort.** The points represent the *trans*-eQTL effect size estimates from regenie and the error bars represent 95% confidence intervals.

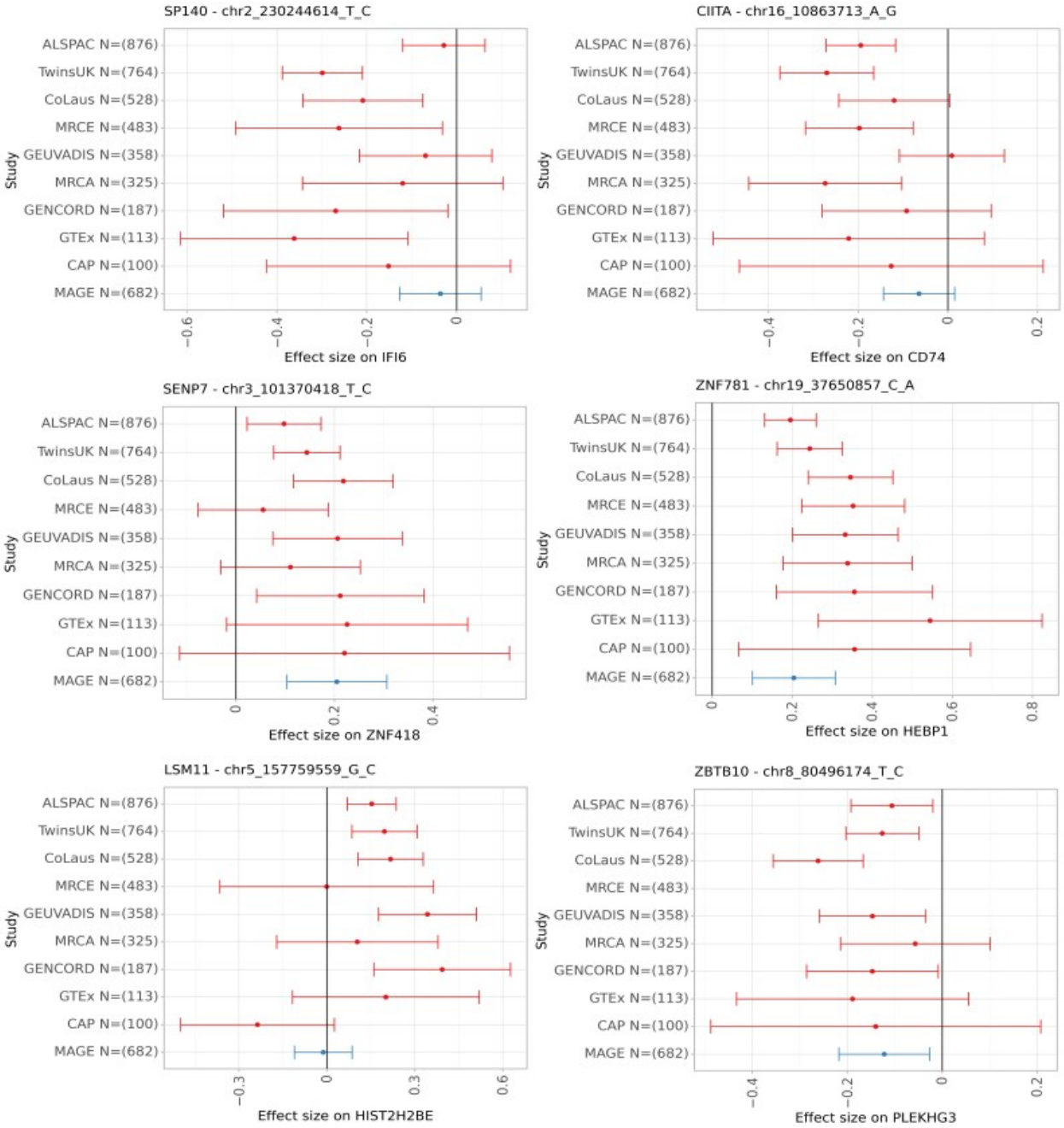

Figure S3. **Forest plots showing cohort-specific effect size for the remaining *trans*-eQTL loci that either did not replicate in the MAGE cohort or corresponded to likely cross-mappability artefacts (*SENP7*, *ZNF781* and *ZBTB10* loci).** The points represent the *trans*-eQTL effect size estimates from regenie and the error bars represent 95% confidence intervals.

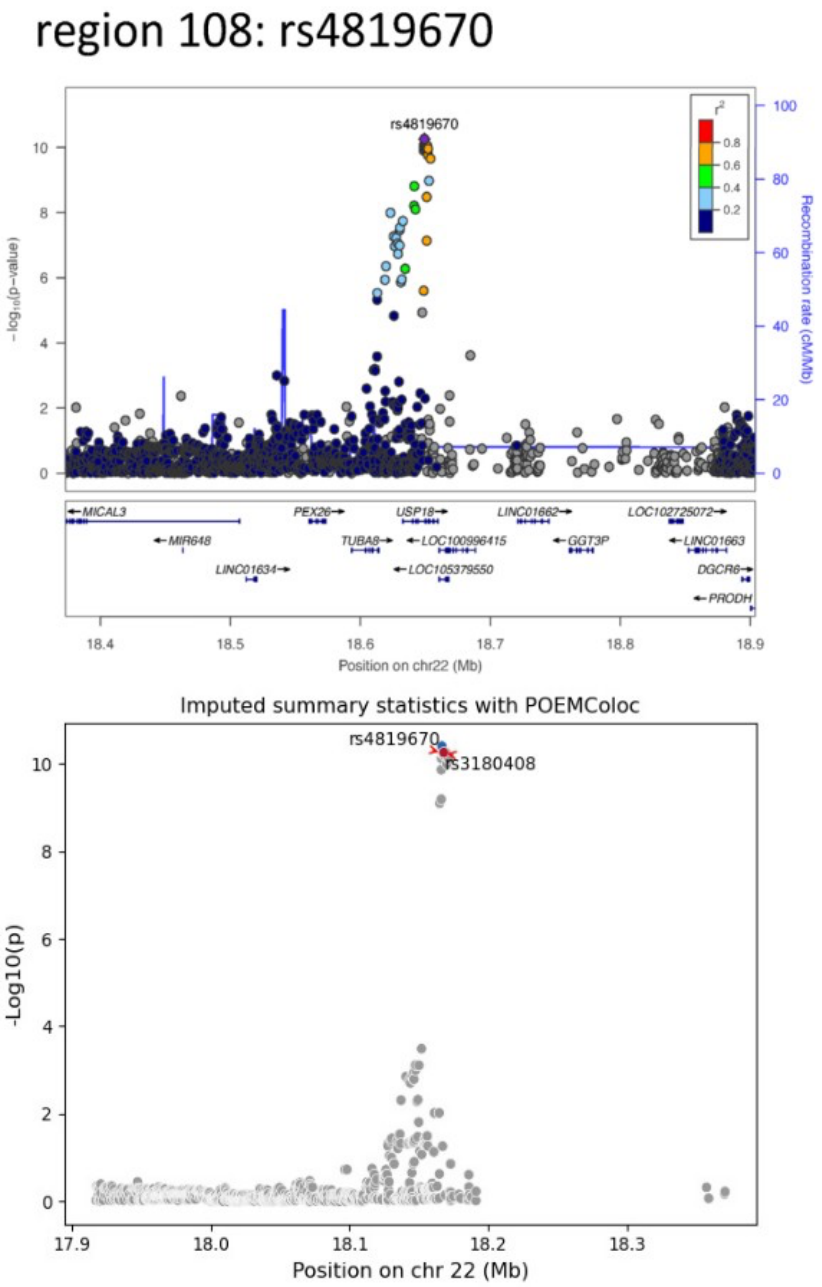

Figure S4. Original regional association plot for the *USP18* SLE GWAS locus from Yin *et al.* 2020 study (top panel) and the summary statistics imputed with POEMColoc for the same locus (bottom panel).

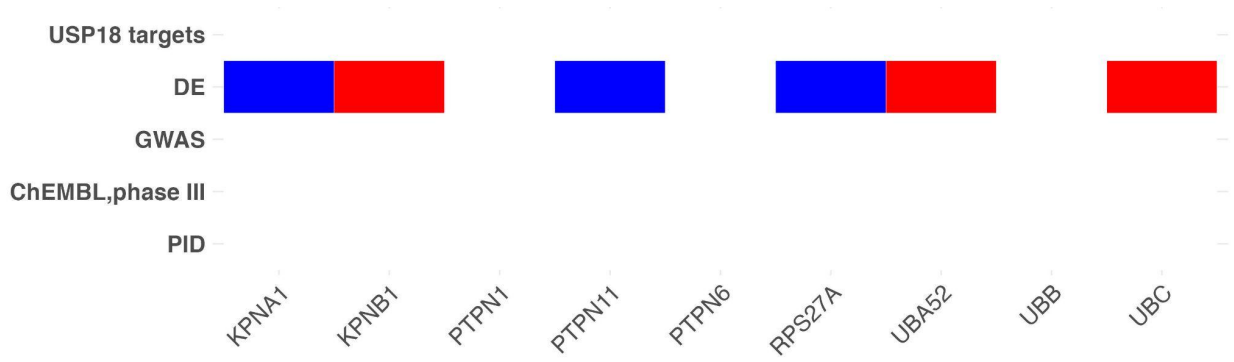

Figure S5. Category III: other interferon alpha/beta signalling pathway genes that do not belong to categories I or II (shown in Figure 3). The increased gene expression is marked in red, while reduced gene expression is marked in blue. The visualisation illustrates the effect on USP18 targets in relation to the risk allele. DE - differential gene expression in SLE cases *versus* controls[43]; GWAS - GWAS hits for SLE[33], ChEMBL, phase III - SLE phase III clinical trials from ChEMBL[50], PID - genes causing primary immunodeficiency from Genomics England.

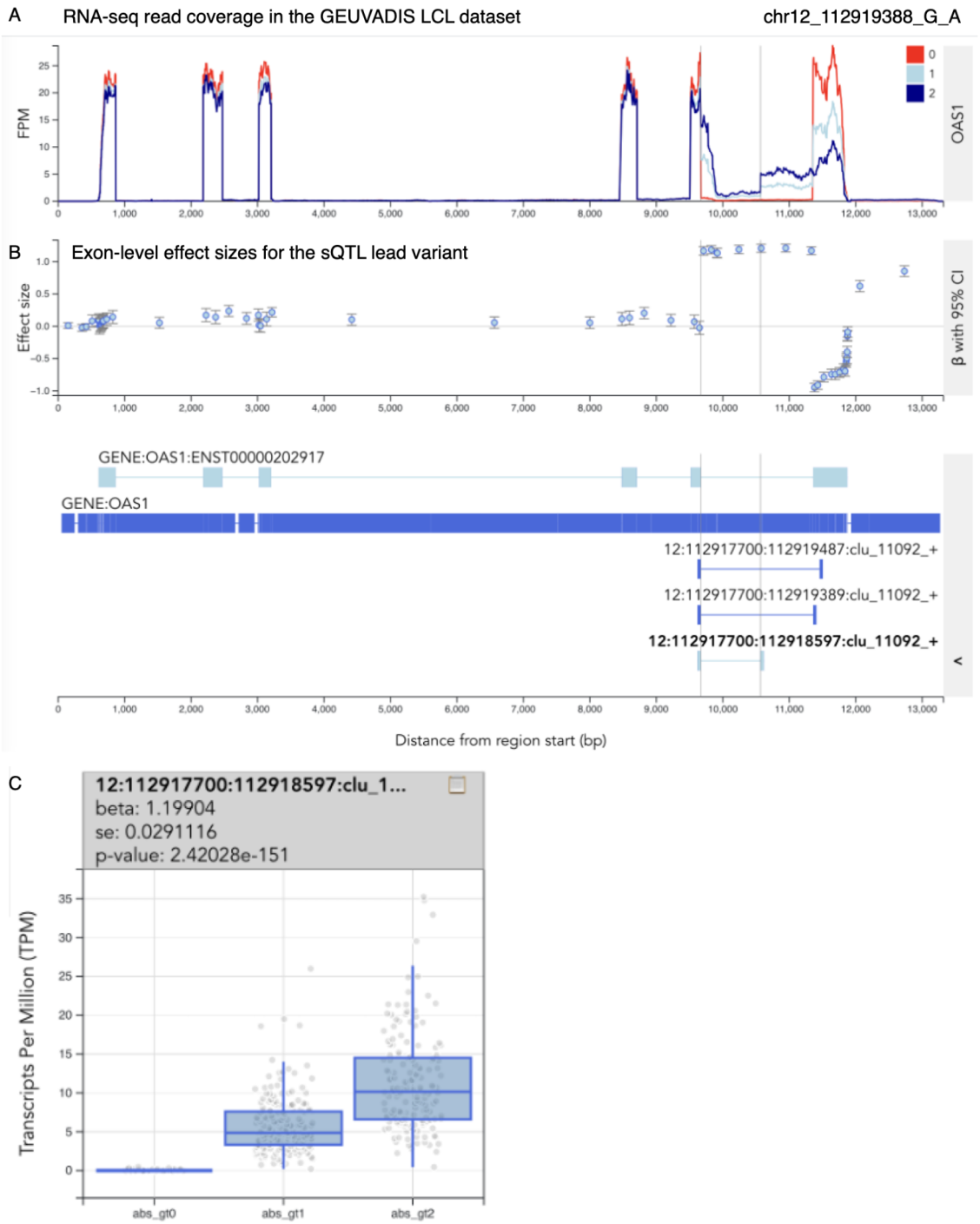

Figure S6. Fine-mapped splicing QTL (sQTL) in the *OAS1* gene. (**A**) RNA-seq read coverage of the *OAS1* gene in the GEUVADIS LCL dataset, stratified by the genotype of the fine-mapped sQTL variant chr12_112919388_G_A (posterior inclusion probability = 1). (**B**) Exon-level effect sizes for the sQTL lead variant. (**C**) Boxplot of the absolute expression of the short last intron of the *OAS1* gene (highlighted on panel A) stratified by the genotype of the lead sQTL variant. Interactive version of the plot can be viewed here.

990

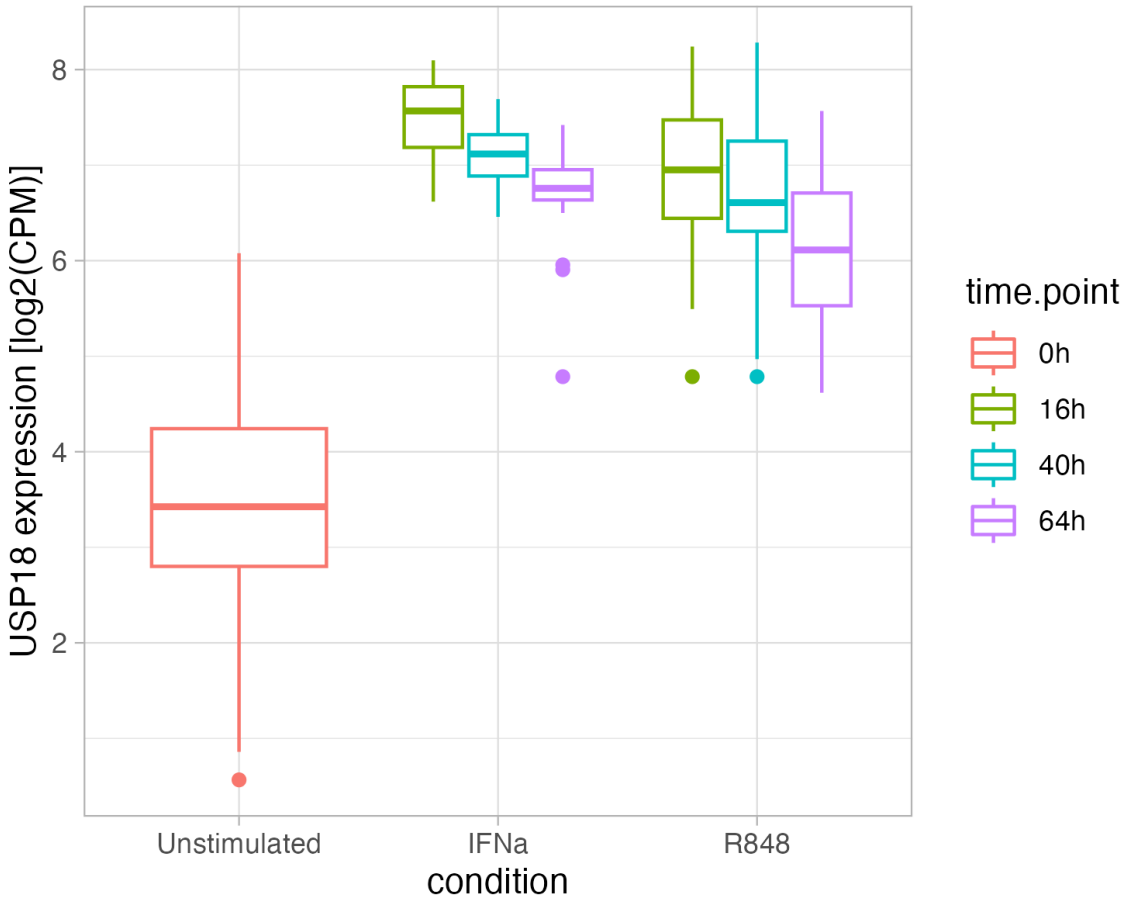

991
992 **Figure S7**. **Expression level of *USP18* in resting and stimulated B-cell subset of**
993 **peripheral blood mononuclear cells (PBMCs)**. PBMCs were isolated from healthy donors and
994 stimulated with interferon-alpha (IFNa) or R848 for 16, 40 and 64 hours.

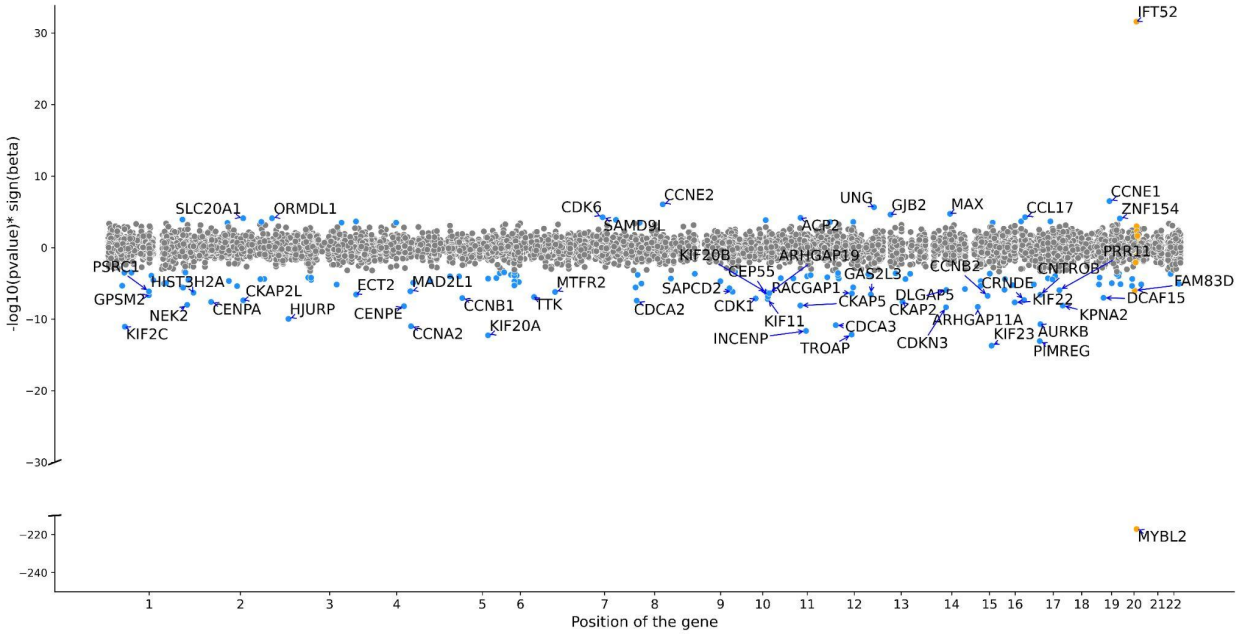

Figure S8. **MYBL2 regulates the expression of many cell cycle genes.** The scatter plot shows all genes associated with the *MYBL2 trans*-eQTL lead variant (chr20_43721344_C_T). Light blue points show significantly associated genes (variant-level Benjamini-Hochberg FDR 5%)

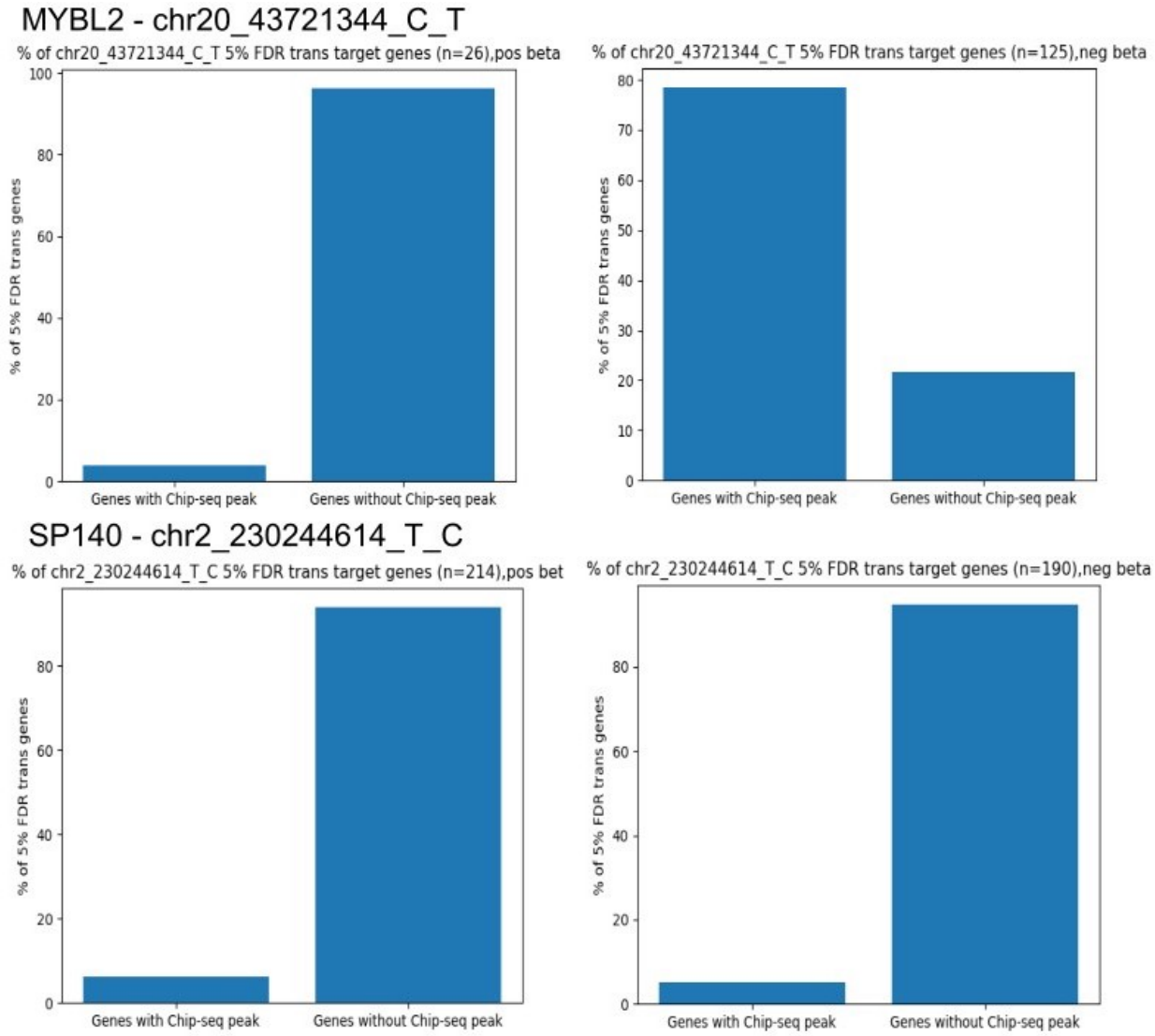

Figure S9. Overlap between *trans*-eQTL target genes and MYBL2 ChIP-seq peaks. The top panel shows the proportion of the *MYBL2 trans*-eQTL target genes upregulated (left) or downregulated (right) by the effect allele that contain a MYBL2 ChIP-seq peak within +/- 2kb from the annotated promoter. The bottom panel shows the proportion of the *SP140 trans*-eQTL target genes upregulated (left) or downregulated (right) by the effect allele that contain a MYBL2 ChIP-seq peak within +/- 2kb from the annotated promoter. Only genes downregulated by the MYBL2 effect allele show a sizable overlap with MYBL2 ChIP-seq peaks.

1012 # References

1013 1. Aguet, F. *et al.* Molecular quantitative trait loci. *Nature Reviews Methods Primers* **3**, 1–22
1014 (2023).
1015 2. Bauer, D. E. *et al.* An erythroid enhancer of BCL11A subject to genetic variation determines
1016 fetal hemoglobin level. *Science* **342**, 253–257 (2013).
1017 3. Frangoul, H. *et al.* CRISPR-Cas9 Gene Editing for Sickle Cell Disease and β-Thalassemia.
1018 *N. Engl. J. Med.* **384**, 252–260 (2021).
1019 4. Liu, X., Li, Y. I. & Pritchard, J. K. Trans Effects on Gene Expression Can Drive Omnigenic
1020 Inheritance. *Cell* **177**, 1022–1034.e6 (2019).
1021 5. Sun, B. B. *et al.* Plasma proteomic associations with genetics and health in the UK
1022 Biobank. *Nature* 1–10 (2023).
1023 6. Võsa, U. *et al.* Large-scale cis- and trans-eQTL analyses identify thousands of genetic loci
1024 and polygenic scores that regulate blood gene expression. *Nat. Genet.* **53**, 1300–1310
1025 (2021).
1026 7. Westra, H.-J. *et al.* Systematic identification of trans eQTLs as putative drivers of known
1027 disease associations. *Nat. Genet.* **45**, 1238–1243 (2013).
1028 8. Ferkingstad, E. *et al.* Large-scale integration of the plasma proteome with genetics and
1029 disease. *Nat. Genet.* **53**, 1712–1721 (2021).
1030 9. Sun, B. B. *et al.* Genomic atlas of the human plasma proteome. *Nature* **558**, 73–79 (2018).
1031 10. Pietzner, M. *et al.* Mapping the proteo-genomic convergence of human diseases. *Science*
1032 **374**, eabj1541 (2021).
1033 11. Bonder, M. J. *et al.* Identification of rare and common regulatory variants in pluripotent cells
1034 using population-scale transcriptomics. *Nat. Genet.* **53**, 313–321 (2021).
1035 12. Kolberg, L., Kerimov, N., Peterson, H. & Alasoo, K. Co-expression analysis reveals
1036 interpretable gene modules controlled by trans-acting genetic variants. *Elife* **9**, e58705

1037 (2020).
1038 13. Kasela, S. *et al.* Pathogenic implications for autoimmune mechanisms derived by
1039 comparative eQTL analysis of CD4+ versus CD8+ T cells. *PLoS Genet.* **13**, e1006643
1040 (2017).
1041 14. Fairfax, B. P. *et al.* Innate immune activity conditions the effect of regulatory variants upon
1042 monocyte gene expression. *Science* **343**, 1246949 (2014).
1043 15. Brandt, M. *et al.* An autoimmune disease risk variant: A trans master regulatory effect
1044 mediated by IRF1 under immune stimulation? *PLoS Genet.* **17**, e1009684 (2021).
1045 16. Small, K. S. *et al.* Identification of an imprinted master trans regulator at the KLF14 locus
1046 related to multiple metabolic phenotypes. *Nat. Genet.* **43**, 561–564 (2011).
1047 17. Consortium, T. G. *et al.* The GTEx Consortium atlas of genetic regulatory effects across
1048 human tissues. *Science* **369**, 1318–1330 (2020).
1049 18. Yazar, S. *et al.* Single-cell eQTL mapping identifies cell type-specific genetic control of
1050 autoimmune disease. *Science* **376**, eabf3041 (2022).
1051 19. Small, K. S. *et al.* Regulatory variants at KLF14 influence type 2 diabetes risk via a female-
1052 specific effect on adipocyte size and body composition. *Nat. Genet.* **50**, 572–580 (2018).
1053 20. Claussnitzer, M. *et al.* FTO Obesity Variant Circuitry and Adipocyte Browning in Humans.
1054 *N. Engl. J. Med.* **373**, 895–907 (2015).
1055 21. Smemo, S. *et al.* Obesity-associated variants within FTO form long-range functional
1056 connections with IRX3. *Nature* **507**, 371–375 (2014).
1057 22. Young, L. S. & Rickinson, A. B. Epstein-Barr virus: 40 years on. *Nat. Rev. Cancer* **4**, 757–
1058 768 (2004).
1059 23. Bjornevik, K. *et al.* Longitudinal analysis reveals high prevalence of Epstein-Barr virus
1060 associated with multiple sclerosis. *Science* **375**, 296–301 (2022).
1061 24. Bar-Or, A. *et al.* Epstein-Barr Virus in Multiple Sclerosis: Theory and Emerging
1062 Immunotherapies. *Trends Mol. Med.* **26**, 296–310 (2020).

1063 25. James, J. A. *et al.* An increased prevalence of Epstein-Barr virus infection in young patients
1064 suggests a possible etiology for systemic lupus erythematosus. *J. Clin. Invest.* **100**, 3019–
1065 3026 (1997).
1066 26. Harley, J. B. *et al.* Transcription factors operate across disease loci, with EBNA2 implicated
1067 in autoimmunity. *Nat. Genet.* **50**, 699–707 (2018).
1068 27. Lanz, T. V. *et al.* Clonally expanded B cells in multiple sclerosis bind EBV EBNA1 and
1069 GlialCAM. *Nature* **603**, 321–327 (2022).
1070 28. Thomas, O. G. *et al.* Heightened Epstein-Barr virus immunity and potential cross-
1071 reactivities in multiple sclerosis. *PLoS Pathog.* **20**, e1012177 (2024).
1072 29. Saha, A. & Battle, A. False positives in trans-eQTL and co-expression analyses arising
1073 from RNA-sequencing alignment errors. *F1000Res.* **7**, 1860 (2018).
1074 30. Taylor, D. J. *et al.* Sources of gene expression variation in a globally diverse cohort. *bioRxiv*
1075 2023.11.04.565639 (2023) doi:10.1101/2023.11.04.565639.
1076 31. Bryois, J. *et al.* Cis and trans effects of human genomic variants on gene expression. *PLoS*
1077 *Genet.* **10**, e1004461 (2014).
1078 32. Mountjoy, E. *et al.* An open approach to systematically prioritize causal variants and genes
1079 at all published human GWAS trait-associated loci. *Nat. Genet.* 1–7 (2021).
1080 33. Yin, X. *et al.* Meta-analysis of 208370 East Asians identifies 113 susceptibility loci for
1081 systemic lupus erythematosus. *Ann. Rheum. Dis.* **80**, 632–640 (2021).
1082 34. King, E. A., Dunbar, F., Davis, J. W. & Degner, J. F. Estimating colocalization probability
1083 from limited summary statistics. *BMC Bioinformatics* **22**, 254 (2021).
1084 35. Kerimov, N. *et al.* eQTL Catalogue 2023: New datasets, X chromosome QTLs, and
1085 improved detection and visualisation of transcript-level QTLs. *PLoS Genet.* **19**, e1010932
1086 (2023).
1087 36. Meuwissen, M. E. C. *et al.* Human USP18 deficiency underlies type 1 interferonopathy
1088 leading to severe pseudo-TORCH syndrome. *J. Exp. Med.* **213**, 1163–1174 (2016).

1089 37. Alsohime, F. *et al.* JAK Inhibitor Therapy in a Child with Inherited USP18 Deficiency. *N.*
1090 *Engl. J. Med.* **382**, 256–265 (2020).
1091 38. McLaren, W. *et al.* The Ensembl Variant Effect Predictor. *Genome Biol.* **17**, 122 (2016).
1092 39. de Lange, K. M. *et al.* Genome-wide association study implicates immune activation of
1093 multiple integrin genes in inflammatory bowel disease. *Nat. Genet.* **49**, 256–261 (2017).
1094 40. Schnitzler, G. R. *et al.* Convergence of coronary artery disease genes onto endothelial cell
1095 programs. *Nature* 1–9 (2024).
1096 41. Weeks, E. M. *et al.* Leveraging polygenic enrichments of gene features to predict genes
1097 underlying complex traits and diseases. *Nat. Genet.* **55**, 1267–1276 (2023).
1098 42. Mostafavi, S. *et al.* Parsing the Interferon Transcriptional Network and Its Disease
1099 Associations. *Cell* **164**, 564–578 (2016).
1100 43. Banchereau, R. *et al.* Personalized Immunomonitoring Uncovers Molecular Networks that
1101 Stratify Lupus Patients. *Cell* **165**, 551–565 (2016).
1102 44. Baechler, E. C. *et al.* Interferon-inducible gene expression signature in peripheral blood
1103 cells of patients with severe lupus. *Proc. Natl. Acad. Sci. U. S. A.* **100**, 2610–2615 (2003).
1104 45. Jefferies, C. A. Regulating IRFs in IFN Driven Disease. *Front. Immunol.* **10**, 325 (2019).
1105 46. Honda, K., Takaoka, A. & Taniguchi, T. Type I interferon [corrected] gene induction by the
1106 interferon regulatory factor family of transcription factors. *Immunity* **25**, 349–360 (2006).
1107 47. Reshef, Y. A. *et al.* Detecting genome-wide directional effects of transcription factor binding
1108 on polygenic disease risk. *Nat. Genet.* **50**, 1483–1493 (2018).
1109 48. Li, H. *et al.* Identification of a Sjögren's syndrome susceptibility locus at OAS1 that
1110 influences isoform switching, protein expression, and responsiveness to type I interferons.
1111 *PLoS Genet.* **13**, e1006820 (2017).
1112 49. Banday, A. R. *et al.* Genetic regulation of OAS1 nonsense-mediated decay underlies
1113 association with COVID-19 hospitalization in patients of European and African ancestries.
1114 *Nat. Genet.* **54**, 1103–1116 (2022).

1115 50. Zdrazil, B. *et al.* The ChEMBL Database in 2023: a drug discovery platform spanning
1116 multiple bioactivity data types and time periods. *Nucleic Acids Res.* **52**, D1180–D1192
1117 (2024).
1118 51. Morand, E. F. *et al.* Trial of Anifrolumab in Active Systemic Lupus Erythematosus. *N. Engl.*
1119 *J. Med.* **382**, 211–221 (2020).
1120 52. Amaya-Uribe, L., Rojas, M., Azizi, G., Anaya, J.-M. & Gershwin, M. E. Primary
1121 immunodeficiency and autoimmunity: A comprehensive review. *J. Autoimmun.* **99**, 52–72
1122 (2019).
1123 53. Schmidt, R. E., Grimbacher, B. & Witte, T. Autoimmunity and primary immunodeficiency:
1124 two sides of the same coin? *Nat. Rev. Rheumatol.* **14**, 7–18 (2017).
1125 54. Ghodke-Puranik, Y., Olferiev, M. & Crow, M. K. Systemic lupus erythematosus genetics:
1126 insights into pathogenesis and implications for therapy. *Nat. Rev. Rheumatol.* **20**, 635–648
1127 (2024).
1128 55. Primary immunodeficiency or monogenic inflammatory bowel disease (Version 4.191).
1129 https://panelapp.genomicsengland.co.uk/panels/398/.
1130 56. Crow, M. K. Advances in lupus therapeutics: Achieving sustained control of the type I
1131 interferon pathway. *Curr. Opin. Pharmacol.* **67**, 102291 (2022).
1132 57. Mackensen, A. *et al.* Anti-CD19 CAR T cell therapy for refractory systemic lupus
1133 erythematosus. *Nat. Med.* **28**, 2124–2132 (2022).
1134 58. Müller Fabian *et al.* CD19 CAR T-Cell Therapy in Autoimmune Disease — A Case Series
1135 with Follow-up. *N. Engl. J. Med.* **390**, 687–700 (2024).
1136 59. Akinbiyi, T., McPeek, M. S. & Abney, M. ADELLE: A global testing method for Trans-eQTL
1137 mapping. *bioRxiv* 2024.02.24.581871 (2024) doi:10.1101/2024.02.24.581871.
1138 60. Dutta, D. *et al.* Aggregative trans-eQTL analysis detects trait-specific target gene sets in
1139 whole blood. *Nat. Commun.* **13**, 1–14 (2022).
1140 61. Wang, L., Babushkin, N., Liu, Z. & Liu, X. Trans-eQTL mapping in gene sets identifies

network effects of genetic variants. *bioRxiv* 2022.11.11.516189 (2022) doi:10.1101/2022.11.11.516189.

62. Wang, Y.-F. *et al.* Identification of 38 novel loci for systemic lupus erythematosus and genetic heterogeneity between ancestral groups. *Nat. Commun.* **12**, 772 (2021).
63. McNab, F., Mayer-Barber, K., Sher, A., Wack, A. & O'Garra, A. Type I interferons in infectious disease. *Nat. Rev. Immunol.* **15**, 87–103 (2015).
64. Interleukin-6 Receptor Mendelian Randomisation Analysis (IL6R MR) Consortium *et al.* The interleukin-6 receptor as a target for prevention of coronary heart disease: a mendelian randomisation analysis. *Lancet* **379**, 1214–1224 (2012).
65. C Reactive Protein Coronary Heart Disease Genetics Collaboration (CCGC) *et al.* Association between C reactive protein and coronary heart disease: mendelian randomisation analysis based on individual participant data. *BMJ* **342**, d548 (2011).
66. Burgess, S. *et al.* Using genetic association data to guide drug discovery and development: Review of methods and applications. *Am. J. Hum. Genet.* **110**, 195–214 (2023).
67. Zheng, J. *et al.* Phenome-wide Mendelian randomization mapping the influence of the plasma proteome on complex diseases. *Nat. Genet.* **52**, 1122–1131 (2020).
68. Karim, M. A. *et al.* Systematic disease-agnostic identification of therapeutically actionable targets using the genetics of human plasma proteins. *medRxiv* (2023) doi:10.1101/2023.06.01.23290252.
69. Wong, D. *et al.* Genomic mapping of the MHC transactivator CIITA using an integrated ChIP-seq and genetical genomics approach. *Genome Biol.* **15**, 494 (2014).
70. Civelek, M. *et al.* Genetic Regulation of Adipose Gene Expression and Cardio-Metabolic Traits. *Am. J. Hum. Genet.* **100**, 428–443 (2017).
71. Hore, V. *et al.* Tensor decomposition for multiple-tissue gene expression experiments. *Nat. Genet.* **48**, 1094–1100 (2016).
72. Ntranos, V., Kamath, G. M., Zhang, J. M., Pachter, L. & Tse, D. N. Fast and accurate

1167 single-cell RNA-seq analysis by clustering of transcript-compatibility counts. *Genome Biol.*
1168 **17**, 112 (2016).
1169 73. EQTLGen consortium. https://www.eqtlgen.org/.
1170 74. Morris, J. A. *et al.* Discovery of target genes and pathways at GWAS loci by pooled single-
1171 cell CRISPR screens. *Science* **380**, eadh7699 (2023).
1172 75. Weinstock, J. S. *et al.* Gene regulatory network inference from CRISPR perturbations in
1173 primary CD4+ T cells elucidates the genomic basis of immune disease. *bioRxiv*
1174 2023.09.17.557749 (2023) doi:10.1101/2023.09.17.557749.
1175 76. Boyd, A. *et al.* Cohort Profile: the 'children of the 90s'--the index offspring of the Avon
1176 Longitudinal Study of Parents and Children. *Int. J. Epidemiol.* **42**, 111–127 (2013).
1177 77. Fraser, A. *et al.* Cohort Profile: the Avon Longitudinal Study of Parents and Children:
1178 ALSPAC mothers cohort. *Int. J. Epidemiol.* **42**, 97–110 (2013).
1179 78. Buil, A. *et al.* Gene-gene and gene-environment interactions detected by transcriptome
1180 sequence analysis in twins. *Nat. Genet.* **47**, 88–91 (2015).
1181 79. Firmann, M. *et al.* The CoLaus study: a population-based study to investigate the
1182 epidemiology and genetic determinants of cardiovascular risk factors and metabolic
1183 syndrome. *BMC Cardiovasc. Disord.* **8**, 6 (2008).
1184 80. Sönmez Flitman, R. *et al.* Untargeted Metabolome- and Transcriptome-Wide Association
1185 Study Suggests Causal Genes Modulating Metabolite Concentrations in Urine. *J. Proteome*
1186 *Res.* **20**, 5103–5114 (2021).
1187 81. Lappalainen, T. *et al.* Transcriptome and genome sequencing uncovers functional variation
1188 in humans. *Nature* **501**, 506–511 (2013).
1189 82. Liang, L. *et al.* A cross-platform analysis of 14,177 expression quantitative trait loci derived
1190 from lymphoblastoid cell lines. *Genome Res.* **23**, 716–726 (2013).
1191 83. Gutierrez-Arcelus, M. *et al.* Passive and active DNA methylation and the interplay with
1192 genetic variation in gene regulation. *Elife* **2**, e00523 (2013).

1193 84. Theusch, E., Chen, Y.-D. I., Rotter, J. I., Krauss, R. M. & Medina, M. W. Genetic variants
1194 modulate gene expression statin response in human lymphoblastoid cell lines. *BMC*
1195 *Genomics* **21**, 555 (2020).
1196 85. Zhao, H. *et al.* CrossMap: a versatile tool for coordinate conversion between genome
1197 assemblies. *Bioinformatics* **30**, 1006–1007 (2014).
1198 86. Byrska-Bishop, M. *et al.* High-coverage whole-genome sequencing of the expanded 1000
1199 Genomes Project cohort including 602 trios. *Cell* **185**, 3426–3440.e19 (2022).
1200 87. Deelen, P. *et al.* Genotype harmonizer: automatic strand alignment and format conversion
1201 for genotype data integration. *BMC Res. Notes* **7**, 901 (2014).
1202 88. Taliun, D. *et al.* Sequencing of 53,831 diverse genomes from the NHLBI TOPMed Program.
1203 *Nature* **590**, 290–299 (2021).
1204 89. Das, S. *et al.* Next-generation genotype imputation service and methods. *Nat. Genet.* **48**,
1205 1284–1287 (2016).
1206 90. Fuchsberger, C., Abecasis, G. R. & Hinds, D. A. minimac2: faster genotype imputation.
1207 *Bioinformatics* **31**, 782–784 (2015).
1208 91. Loh, P.-R. *et al.* Reference-based phasing using the Haplotype Reference Consortium
1209 panel. *Nat. Genet.* **48**, 1443–1448 (2016).
1210 92. Kerimov, N. *et al.* A compendium of uniformly processed human gene expression and
1211 splicing quantitative trait loci. *Nat. Genet.* **53**, 1290–1299 (2021).
1212 93. Kim, D., Langmead, B. & Salzberg, S. L. HISAT: a fast spliced aligner with low memory
1213 requirements. *Nat. Methods* **12**, 357–360 (2015).
1214 94. Quinlan, A. R. & Hall, I. M. BEDTools: a flexible suite of utilities for comparing genomic
1215 features. *Bioinformatics* **26**, 841–842 (2010).
1216 95. Gautier, L., Cope, L., Bolstad, B. M. & Irizarry, R. A. affy--analysis of Affymetrix GeneChip
1217 data at the probe level. *Bioinformatics* **20**, 307–315 (2004).
1218 96. Mbatchou, J. *et al.* Computationally efficient whole-genome regression for quantitative and

1219 binary traits. *Nat. Genet.* **53**, 1097–1103 (2021).
1220 97. Nica, A. C. *et al.* The architecture of gene regulatory variation across multiple human
1221 tissues: the MuTHER study. *PLoS Genet.* **7**, e1002003 (2011).
1222 98. Storey, J. D. & Tibshirani, R. Statistical significance for genomewide studies. *Proc. Natl.*
1223 *Acad. Sci. U. S. A.* **100**, 9440–9445 (2003).
1224 99. Robinson, M. D. & Oshlack, A. A scaling normalization method for differential expression
1225 analysis of RNA-seq data. *Genome Biol.* **11**, R25 (2010).
1226 100. Roshchupkin, G. V. *et al.* HASE: Framework for efficient high-dimensional association
1227 analyses. *Sci. Rep.* **6**, 36076 (2016).
1228 101. Seabold, S. & Perktold, J. Statsmodels: Econometric and statistical modeling with python.
1229 in *Proceedings of the 9th Python in Science Conference* (SciPy, 2010).
1230 doi:10.25080/majora-92bf1922-011.
1231 102. Huang, Y., McCarthy, D. J. & Stegle, O. Vireo: Bayesian demultiplexing of pooled single-
1232 cell RNA-seq data without genotype reference. *Genome Biol.* **20**, 273 (2019).
1233 103. Hao, Y. *et al.* Integrated analysis of multimodal single-cell data. *Cell* **184**, 3573–3587.e29
1234 (2021).
1235 104. McCarthy, D. J., Chen, Y. & Smyth, G. K. Differential expression analysis of multifactor
1236 RNA-Seq experiments with respect to biological variation. *Nucleic Acids Res.* **40**, 4288–
1237 4297 (2012).
1238 105. Kowalczyk, M. S. *et al.* Single-cell RNA-seq reveals changes in cell cycle and differentiation
1239 programs upon aging of hematopoietic stem cells. *Genome Res.* **25**, 1860–1872 (2015).
1240 106. Hao, Y. *et al.* Dictionary learning for integrative, multimodal and scalable single-cell
1241 analysis. *Nat. Biotechnol.* **42**, 293–304 (2023).

1242